J. Physiol. (1980), **300**, *pp.* 213–250
With 20 text-figures
Printed in Great Britain

TEMPORAL AND SPATIAL CHARACTERISTICS OF THE VOLTAGE RESPONSE OF RODS IN THE RETINA OF THE SNAPPING TURTLE

BY P. B. DETWILER,* A. L. HODGKIN AND P. A. MCNAUGHTON

*From the Physiological Laboratory, University of Cambridge and *the Department of Physiology and Biophysics, School of Medicine, University of Washington, Seattle, U.S.A.*

(*Received 5 June 1979*)

SUMMARY

1. In response to strong, large-field flashes the dark-adapted rods of *Chelydra serpentina* gave initial hyperpolarizing responses of 30–40 mV, declining rapidly to plateaus of 10–15 mV which lasted 20 sec or more.

2. In the most sensitive cells the flash-sensitivity at 520 nm to a large illuminated area was 3–6 mV per photoisomerization (assuming an effective collecting area of 13·6 μm^2).

3. The initial response to a step of light agreed with that predicted by superposition from the flash response but even with very weak lights the step response fell below the predicted curve at times longer than about 2 sec.

4. The step sensitivity defined from the initial peak of the response to a step of light was 2–6 mV photoisomerization^{-1} sec, about 1000 times greater than the most sensitive cones in the turtle retina.

5. The response to a small weakly illuminated spot (radius 21 μm) reached a peak later and lasted longer than the linear response to a weakly illuminated large area (radius 570 μm).

6. The difference in sensitivity between large and small spots was reasonably consistent with the apparent space constant of the rod network obtained from the exponential decline of the flash response on either side of an illuminated strip.

7. As others have found, strong flashes did not give an initial hyperpolarizing transient when the radius of the spot was less than about 50 μm.

8. Experiments made by flashing long narrow strips of light onto the retina showed that the response spread a long way initially ($\lambda \doteqdot 70$ μm) and then contracted down to a relatively small region ($\lambda \doteqdot 25$ μm) at times of about 2 sec. When the line source was at some distance from the impaled rod the response reached a peak earlier and was shorter than when the source was close.

9. The results in (8) can be explained quantitatively by assuming that delayed voltage-dependent conductance changes mimic an inductance and make the rod network behave like a high-pass filter with series resistance and parallel inductance.

10. In sensitive rods, flash responses varied randomly with a variance which was about 1/30 of that expected in an isolated cell; this reduction in noise is satisfactorily explained by electrical coupling between rods.

0022-3751/80/7210-0260 $07.50

11. The variance peak usually occurred later than the potential peak of the rod response.

12. The high-pass filter characteristics of the rod-network help to explain several puzzling features of the behaviour of rods, for example (1), (5), (7), (8) and (11) of this summary.

13. The high-pass filter characteristics of the rod-network may help it to optimize the signal to noise ratio by integrating over a large area for rapid signals and over a small one for slow signals.

INTRODUCTION

In recent years the electrical properties of turtle rods have been studied with microelectrodes by several authors (Schwartz, 1973, 1975, 1976; Copenhagen & Owen, 1976*a*, *b*; Baylor & Hodgkin, 1973, 1974; Lamb & Simon, 1976*a*, *b*). Although there are some quantitative differences between the conclusions of different authors there is agreement about the following general points, which also apply to the rods of other animals, such as *Bufo marinus* (see Fain, 1975, 1976; Fain, Gold & Dowling, 1976; Cervetto, Pasino & Torre, 1977; Gold, 1979): (1) when expressed in volts per photoisomerization the sensitivity of rods is 1–2 orders of magnitude greater than that of cones in the same retina; (2) the electrical response of rods lasts several times longer than that of cones; (3) in rods weak background lights have a striking effect in reducing the sensitivity and shortening the duration of the response to a flash; (4) the desensitization which outlasts a response to a bright flash is much more obvious and prolonged in rods than in cones; (5) rods may be more tightly coupled than cones: in turtle rods electrical interaction can be recorded over 100 μm or more as opposed to 50 μm in cones; (6) electrical coupling between receptors reduces photon noise in both rods and cones; a variability which may result from the random absorption of photons has been observed with internal electrodes in rods but not in cones; (7) the ratio of peak to plateau after a strong flash is larger in rods than in cones; (8) there are differences between the response of rods to large and small spots of light which suggest that the interactions between rods may be somewhat complicated in nature (see Schwartz, 1975, 1976; Copenhagen & Owen, 1976*a*).

The aim of this and a later paper is to provide a quantitative basis for some of these conclusions and to attempt to answer certain questions about the nature of the transduction mechanism. The properties of the desensitization system are considered in a later paper. The present paper deals with the flash and step sensitivities of rods, with the components in the response to strong flashes and with the measurements of the space constant in the rod network; it also contains an account of the unexpected changes in wave form that occur when an illuminated slit is moved away from the impaled rod (Detwiler, Hodgkin & McNaughton, 1978).

METHODS

Animal care

The experiments to be described were carried out on the isolated eyecup of the snapping turtle, *Chelydra serpentina*. Animals with shells 20–35 cm long were shipped via air freight by the Mogul-Ed Company of Oshkosh, Wisconsin. They were kept in the laboratory in a 4 × 7 ft. holding tank that contained water at a depth of about 10 in. and a readily accessible dry plat-

form. The water was recirculated through a charcoal filter and maintained at a temperature of 21–23 °C. It was found that the health of the animals had a marked influence on the quality of the experiments. Consequently, new animals were allowed two to four weeks to recover from shipping. During this time they were fed on ox heart and kept on a light-dark cycle of 16 and 8 hr respectively.

Preparation

An animal selected for an experiment was first dark adapted for 8–12 hr and the isolated eyecup prepared under dim red light using methods similar to those of Baylor, Fuortes & O'Bryan (1971). Following decapitation one eye was removed from the pithed head and cut into anterior and posterior halves. The cut was made on an angle such that the optic disk was closer to the ventral than the dorsal edge of the posterior half. Kleenex wicks were placed on and to the right and to the left of the optic disk to drain the vitreous humor. The eyecup was then placed in a moist recording chamber, ventilated with 95% O_2 and 5% CO_2 at 18–21 °C. The recording chamber was fixed to a movable platform in a light-tight box positioned to receive the output of the optical stimulator. The lid of the box contained a manual shutter that carried on its outside surface a rectangular grid on a microscope reticle.

Stimulation and recording

An optical bench of the Baylor & Hodgkin (1973) design was used to form a reduced image (33 ×) of a variable field aperture on the retina. The intensity and spectral composition of stimuli were controlled using neutral density and narrow band interference filters as described by Baylor & Hodgkin (1973). Light intensity was measured at approximately monthly intervals with a calibrated silicon photodiode (United Detector Technology, Inc. 40 × optometer) placed at the position of the retina. The accuracy of the photodiode was checked with two other calibrated devices of a similar design. The optical density of individual neutral density filters was measured using the same photodiodes, and the addition of several neutral density filters in series checked using a photomultiplier for the higher attenuations.

Intracellular micro-electrodes were drawn from Pyrex Omega Dot tubing (Glass Company of America, Bargaintown, New Jersey) on a Livingston-type horizontal puller. Micro-electrodes were filled with 4 M potassium acetate (pH 7·4) and had resistances in the vitreous of about 200–400 MΩ. Electrodes were connected to a high impedance negative capacitance pre-amplifier (Colburn & Schwartz, 1972). An FM tape recorder with band width of DC to 1250 Hz (Analog 7, Philips, Eindhoven, Holland) was used to record intracellular potential on high and low gain as well as the light stimulus and trigger pulse. For analysis of the time course of the variance and mean of a series of responses, signals from the tape were digitized and stored on a cartridge disk of a DEC PDP11/10 computer (see Lamb & Simon, 1976*a*, *b* for details); weak, slow signals were passed through a low-pass filter set to 50 Hz. In most cases each sweep was sampled 512 times at 10 msec intervals. The mean and variance for each point was then calculated.

Experimental procedure

In order to keep the retina as dark-adapted as possible the following procedure was used to position the recording electrode in the stimulating light spot. A cut-off filter that passed only wave-lengths greater than 800 nm was placed in the path of the optical stimulator. With the shutter in the light-tight box open the stimulus spot was viewed using a silicon vidicon (Akai Model VC-70) coupled to a Wild stereo-microscope. The spot was focused on a selected region of the dorsal retina and its position marked on the screen of the TV monitor. The shutter on the box was then closed and the rectangular grid on the shutter surface illuminated with white light. The TV camera was adjusted vertically to form a focused image of the grid on the monitor. This allowed the mark on the monitor screen that corresponded to the position of the stimulus spot on the retina to be read in grid co-ordinates. The recording electrode was then positioned using the grid co-ordinates. With the grid illuminator off and the box shutter open the electrode was then lowered vertically until it made contact with the retina. This method of electrode positioning had an accuracy of ± 50 μm. When required by experimental design, finer adjustments to spot position could be made after impaling a receptor by using the cell response as an indicator.

Throughout the experiment extreme precautions were taken to shield the retina from stray light. The light-tight box containing the recording chamber was enclosed in a larger black box and the laboratory was dimly lit with red light.

The micro-electrode was advanced into the retina while 20 msec flashes of dim 640 nm light were applied at 6 sec intervals. When the electrode was just past the horizontal cell layer, the wave-length of the stimulus was changed to 520 nm and flashes were applied every 10 sec at an intensity of 0·5 photon μm^{-2} $flash^{-1}$ or less. The electrode was then lowered further to impale a receptor which was identified as a rod on the basis of its absolute sensitivity, spectral sensitivity and response time course.

RESULTS

Responses to weak flashes and steps; sensitivity

Table 1 shows the flash sensitivities of rods determined with large spots of radius 570 μm. In calculating S_F^ϕ, the average voltage per photoisomerization in a rod, we have used Copenhagen & Owen's (1976*a*) value of 13·6 Rh* $photon^{-1}$ μm^2 for the effective collecting area of a rod in *Chelydra*. The average flash sensitivity is about twice that observed by Copenhagen & Owen (1976*a*) and 10 times that found by Schwartz (1975). As suggested by Copenhagen & Owen (1976*a*) it now seems likely that the relatively low sensitivities recorded by Baylor & Hodgkin (1973) on *Pseudemys* or by Schwartz (1975) on *Chelydra* were caused by exposure of the retina to too much light in setting up the experiment. Our experience confirms this, as we recorded much lower sensitivities and shorter times to peak than in Table 1 after accidentally exposing the retina to white light instead of infra-red, when setting up the experiment, for example S_F^ϕ = 0·06 mV $photon^{-1}$ μm^2 and t_{max} = 0·37 sec in one instance. It will be shown in a later paper that although rods in an eyecup preparation recover much of their sensitivity after partial bleaching, they do not return to their initial fully dark-adapted state.

As can be seen from Table 1, a few rods have sensitivities of 3–6 mV $(Rh^*)^{-1}$ that are several times larger than the average. Since this extra sensitivity was not associated with an unusually long response it can probably not be attributed to more complete dark adaptation in these particular rods. One factor that may be important

TABLE 1. Flash sensitivities, times to peak and maximum hyperpolarizations

Number of rods		S_F $\left(\frac{mV\ \mu m^2}{photon}\right)$	S_F^ϕ $\left(\frac{mV}{Rh^*}\right)$	t_{peak} (sec)	U_{max} (mV)
11	Range	43–77	3·1–5·8	0·61–1·10	20–40
	Mean	54	4·0	0·87	32
15	Range	27–36	2·0–2·6	0·65–1·75	20–33
	Mean	30	2·2	1·07	27
32	Range	14–26	1·0–1·9	0·60–1·32	18–37
	Mean	19	1·4	0·92	26
37	Range	7–14	0·50–0·97	0·56–1·79	18–36
	Mean	10	0·74	0·97	25
12	Range	3·0–6·4	0·22–0·47	0·55–1·45	18–31
	Mean	5·4	0·40	0·91	23
Over-all	mean	19·6	1·44	0·95	26·0

Rods have been ordered into five arbitrary groups on the basis of their flash sensitivity. S_F is the flash sensitivity determined with weak flashes at 521 nm from responses of 0·5–2·0 mV; S_F^ϕ gives sensitivity in mV per photoisomerization (Rh*) calculated from S_F by dividing by 13·6 Rh* $photon^{-1}$ μm^2 (see Copenhagen & Owen, 1976); t_{peak} is the time to peak of the linear responses and U_{max} is the peak hyperpolarization to a strong flash. Temperature about 20 °C.

is the physical condition of the animal. Thus six out of the eleven rods in the most sensitive group in Table 1 came from two animals both of which had been fed regularly for many weeks and were exceptionally strong and active.

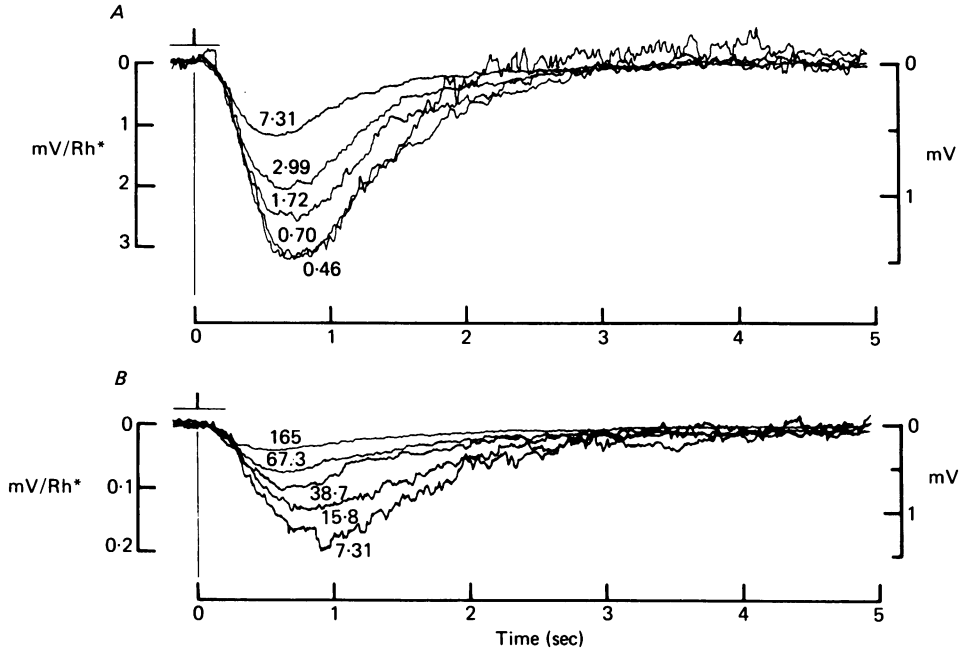

Fig. 1. Scaled amplitudes of responses with large (*A*) and small spots (*B*) – see p. 224 for discussion of *B*.

The abscissa is time after the flash and the ordinate is the change in potential ΔV divided by the number of photoisomerizations (Rh*) per flash in each rod. This number which is shown on each curve was calculated by multiplying the strength of the flash in photon μm^{-2} by a 'collecting area' of 13·6 Rh* photon^{-1} μm^2. The left-hand scale in mV/Rh* applies to all curves; the right-hand scale in mV applies only to the response to the weakest flash. In *A* the spot radius was 570 μm and in *B* it was 21·5 μm. The numbers of sweeps averaged were 11, 18, 2, 2, 1, for the five responses in *A* and 10, 5, 1, 1, 1 in *B*, in both cases going from weakest to strongest flash. The same rod was used in *A* and *B* and in Figs. 3 and 7 which give the full intensity series. Temperature 18·6 °C; resting potential −42 mV; peak hyperpolarization 40 mV; flash duration 20 msec; flash repetition rate 1 in 10 sec or 1 in 20 sec; wave length 520 nm in this and all other experiments. Hyperpolarization shown downwards here and in other figures.

Fig. 1*A* shows that the response varied linearly with flash intensity provided that the stimulus was sufficiently small, in this case less than about 1 photoisomerization per rod. In this rod, where the maximum response to a strong flash was 40 mV in amplitude, the response varied linearly with flash intensity up to an amplitude of 3 mV. In most other rods the deviation from linearity became apparent when the response exceeded 1–2 mV. Fig. 1*B* which was obtained with a small spot will be considered later.

The flash sensitivity determined with a large area is an important quantity because it gives the average sensitivity of an isolated rod to a single photon. This conclusion is obvious if rods are isolated but needs justification if they are electrically coupled.

If a single photoisomerization occurs at rod 0, 0 and injects a peak current i_ϕ into the rod network, it produces a potential $V_{0,0}$ which can be expressed either as

$$V_{0,0} = i_\phi r_{\text{in}} \tag{1.1}$$

where r_{in} is the input resistance of the network, or

$$V_{0,0} = i_{0,0} r_{\text{m}} \tag{1.2}$$

where $i_{0,0}$ is the current which flows through the membrane of rod, 0, 0 and r_{m} is the membrane resistance of each rod. Since all the separate rod currents $i_{0,0}$, $i_{0,1}$, ... $i_{\text{m,n}}$, ... must add to i_ϕ it follows that

$$\sum_{m,n} V_{m,n} = i_\phi r_{\text{m}} \tag{1.3}$$

where m and n are numbers giving the co-ordinates of each rod on the x and y axes.

If in each rod there are on average $\bar{q}$ photoisomerizations the potential averaged over all rods in a large illuminated field is:

$$\bar{V} = i_\phi r_{\text{m}} \bar{q}. \tag{1.4}$$

Hence the flash sensitivity to diffuse illumination is the same as if each rod were isolated from its neighbours.

It is easy to see this result intuitively in the special but unlikely case in which there are exactly $\bar{q}$ photoisomerizations in every rod. In that case the rods are isopotential, so no current flows between them and the potential of each is given by $i_\phi r_{\text{m}} \bar{q}$.

In a resistive network the ratio $r_{\text{in}}/r_{\text{m}}$ which determines $V_{0,0}$ depends on the ratio of the space constant λ to D, the effective distance between rods ($D^{-2} = N$ where N is the number of rods per unit area). The mean value of λ at the peak of the response was about 50 μm and from a figure published by Owen & Copenhagen (1977) D was taken as 20 μm; hence $\lambda/D \doteqdot 2{\cdot}5$. From Fig. 3 of Lamb & Simon (1976*a*) if $\lambda/D = 2{\cdot}5$, $r_{\text{in}}/r_{\text{m}} = 0{\cdot}07$. This means that if $S_{\text{F}}^{\phi} = 5$ mV(Rh*)$^{-1}$ the peak potential produced in a single rod by one photoisomerization in that rod is 350 μV. The rest of the 5 mV is distributed among a large number of rods; in a hexagonal network with $\lambda/D = 2{\cdot}5$ about 2/3 of the voltage is in the sixty-one cells nearest the centre (see Fig. 1 of Detwiler & Hodgkin, 1979).

It will be shown later that the apparent space constant λ and the membrane impedance z_{m} are not constant but decrease with time after a flash. However, provided that the response is in the linear region (less than 1–2 mV) it is still true that the average response $\overline{V^\phi(t)}$ observed under conditions of uniform illumination with an average of one photoisomerization per rod gives the voltage response of an isolated rod $V_{\text{isol}}^{\phi}(t)$ to one photoisomerization. Thus the argument based on eqns. (1.1), (1.2) and (1.3) can be extended to the more general case in which r_{m} is replaced by $f(p)$ where p stands for $\partial/\partial t$ and $f(p)$ is a linear differential equation. The essential point in the more general treatment is that the current in each rod is $V_{m,n}(t)/f(p)$ and since $f(p)$ is the same for all rods it can be taken outside the summation signs in eqn. (1.3). Hence, it follows that the mean potential response to a large field flash which delivers an average of 1 photon per rod is related to the rod photocurrent $i^\phi(t)$ by

$$\overline{V^\phi(t)} = i^\phi(t) f(p). \tag{1.5}$$

Hence

$$\overline{V^{\phi}(t)} = V^{\phi}_{\text{isol}}(t). \tag{1.6}$$

Response to steps of light

In cones the response to a very weak step of light is the integral of the response to a weak flash (Baylor & Hodgkin, 1973). In principle one would expect the same result to hold for rods since there should be some low level of light intensity at which photons are absorbed at such a slow rate that their effects do not interact. We were unable to demonstrate this result in rods since the potential sags from the maximum with any response large enough to be seen against the low frequency electrode noise and drift in the record of membrane potential in darkness. However, as can be seen in Fig. 2, superposition holds for the first 1–2 sec. of the step response and the maximum approaches that calculated from superposition. In the most sensitive rods the response

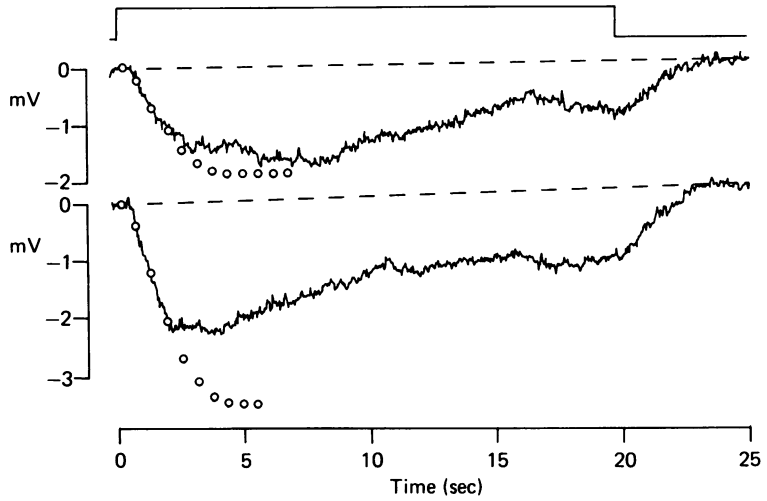

Fig. 2. Failure of superposition. The continuous 'noisy' curves give the response to a rectangular pulse of light, 19·8 sec in duration and of intensity 0·93 Rh* sec^{-1} (upper curve) or 1·80 Rh* sec^{-1} (lower curve). The circles were calculated by integrating the responses to a 20 msec flash of strength 2·0 Rh* and scaling the resulting curve by the appropriate factor. Further details of this rod are given in Table 2 (rod 3). The peak hyperpolarization to a strong flash was 29 mV.

TABLE 2. Step sensitivities and related quantities

Rod	S^{ϕ}_{F} mV/Rh*	t_{peak} sec	t_i sec	S^{ϕ}_{S} observed ← mV(Rh*)$^{-1}$ sec →	S^{ϕ}_{S} calculated
1	4·0	0·94	1·72	5·8	6·9
2	2·3	0·80	1·76	2·6	4·0
3	0·84	1·36	2·31	1·7	1·96
4	1·1	0·84	1·62	1·65	1·74
5	0·38	1·4	1·93	0·53	0·73

S^{ϕ}_{F} is the flash sensitivity; t_{peak}, time to peak and t_i, integration time of flash response S^{ϕ}_{S} is the step sensitivity defined as peak hyperpolarization ÷ by intensity of step. In the last column S^{ϕ}_{S} was calculated as $S^{\phi}_{F}\, t_i$.

started to deviate from that expected on superposition when each rod should on average have contained one molecule of isomerized photopigment. Table 2 gives calculated and observed values of the modified step sensitivity S_s^ϕ defined as peak hyperpolarization/light intensity. The Table shows that the highest values of step sensitivity are about 1000 times greater than in red sensitive cones, i.e. 5 mV $(Rh^*)^{-1}$ sec in rods and 5 μV $(Rh^*)^{-1}$ sec in cones excited with optimally directed light (see Baylor & Hodgkin, 1973; Baylor & Fettiplace, 1975).

The response of rods to flashes and steps: large spots

The three families of curves in Fig. 3, which is from the same experiment as Fig. 1, show how the response changed in shape as the flash was increased from 0·5 Rh* per rod to 19000 Rh* per rod. At the end of the experiment the flash sensitivity returned to its original level of S_f^ϕ = 3·2 mV $(Rh^*)^{-1}$. The main features of this intensity series, some of which have been described by previous authors (Schwartz, 1975; Copenhagen & Owen, 1976*a*; Cervetto *et al.* 1977) are as follows.

(1) Increasing the intensity of the flash from 1 Rh* to 19000 Rh* per rod shortened the time to peak from 0·7 to 0·2 sec.

(2) The initial peak of 40 mV was followed by a slowly declining plateau of amplitude 10–20 mV lasting as much as 20 sec.

(3) The plateau, but not the initial spike, seemed to saturate at a flash strength of about 1000 Rh* per rod. The slow increase in spike amplitude with flash intensity up to 19000 Rh* per rod probably reflects the same phenomenon as the 'lobe' in the amplitude–log intensity curves described by Copenhagen & Owen (1976*a*, Text-fig. 5).

These features were present in all intensity series obtained on rods but there was some quantitative variation. Thus the spike to plateau ratio was often smaller than in the experiment of Fig. 3 and the time to maximum of the linear response was usually longer than in that experiment. In less sensitive cells the duration of the plateau produced by strong flashes was less than in Fig. 3.

Still stronger or longer flashes produced a plateau which might last for many minutes. Recovery from these flashes took place with a time constant of about 8 min. and was incomplete (P. B. Detwiler *et al.* in preparation).

The nature of the spike and plateau

The responses in Fig. 3 are clearly very similar to those described by Cervetto *et al.* (1977) for the rods of *Bufo marinus*. Cervetto *et al.* attribute the decline from the plateau to a desensitization mechanism, rather than to a delayed increase in a voltage dependent conductance of the kind postulated by Baylor, Hodgkin & Lamb (1974*b*) (see also Schwartz, 1976). The reason why they rejected Baylor and colleagues' assumption was that the decline from spike to plateau took place within a voltage range where the input resistance of the rod array was nearly constant. Cervetto *et al.* obtained an excellent fit to their experimental results and their theory may well be partly right. However, the reason for dismissing a voltage-sensitive conductance is not compelling, because the input resistance, r_{in}, of a two-dimensional network varies only very slightly with the membrane resistance r_m; thus r_{in} is approximately proportional to $r_m^{\frac{1}{2}}$ for a tightly coupled network (Jack, Noble & Tsien, 1975; Lamb, 1976).

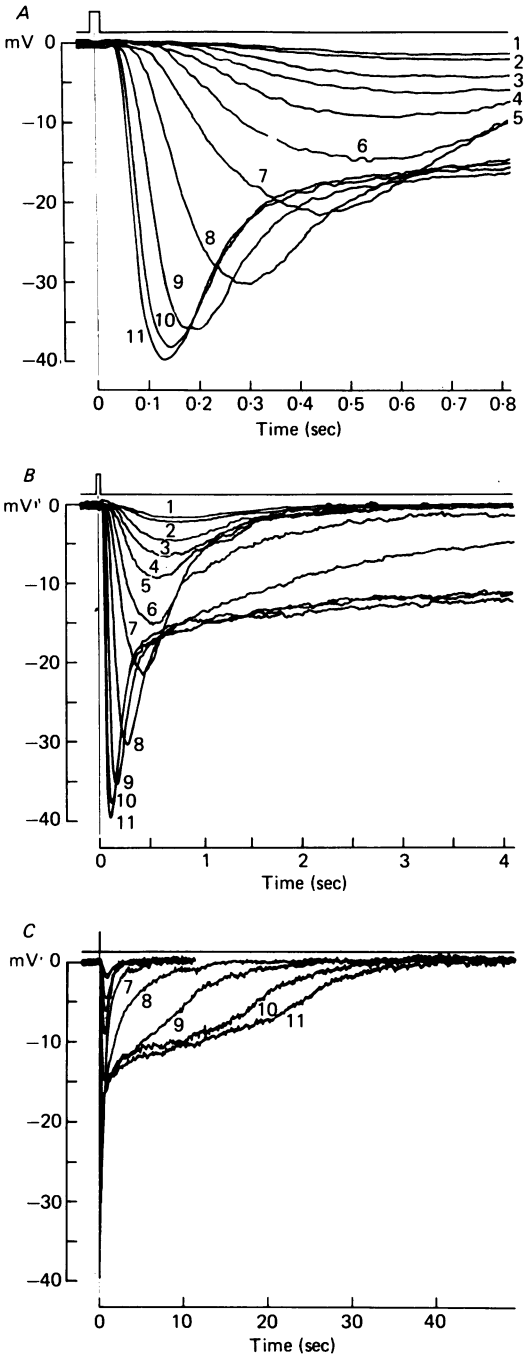

Fig. 3. Intensity series, on three time scales, determined with a large spot (radius 570μm). The curves are from the same series as Fig. 1 and show the responses to 20 msec flashes of strengths given below in Rh*/rod. Curves 1–4; 0·46, 0·70, 1·7, 3·0; Curves 5–8; 7·3, 16, 39, 165; Curves 9–11; 950, 4050, 18900. Experimental details as in Fig. 1. A similar series for a 21·5 μm radius spot from the same rod is given in Fig. 9.

A further argument is that Owen & Copenhagen's (1977) results provide evidence of voltage and time-dependent increases of membrane conductance in the rods of *Chelydra*.

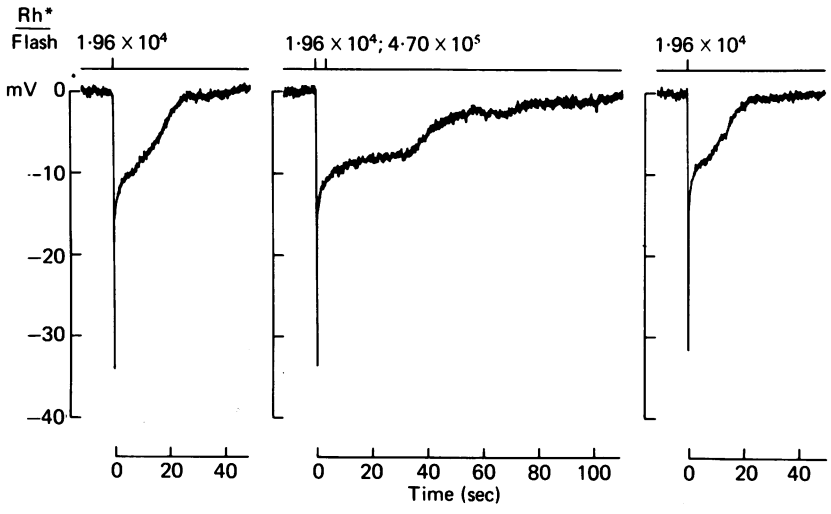

Fig. 4. Records showing that a strong flash delivered during the plateau had no immediate effect but did prolong the plateau. The duration of the flashes was 20 msec and the strength either $1{\cdot}96 \times 10^4$ Rh*/rod (first single flash) or $4{\cdot}7 \times 10^5$ Rh*/rod second flash in middle record).

Fig. 4 illustrates an experiment designed to test whether a rod is completely saturated during the plateau phase, i.e. whether all the light sensitive ionic channels in the outer segment are still closed, or whether some have opened because the system has been desensitized. In the first but not the second case, a strong flash applied during the plateau should have no immediate effect. Fig. 4 and other experiments show that the second flash had no immediate detectable effect even though nearly a million times stronger than that required to give a detectable response in a dark-adapted preparation. This is consistent with the type of model discussed by Baylor, Hodgkin & Lamb (1974*b*), as is the fact that although the second flash had no immediate effect it did greatly prolong the response to the first, weaker flash. These effects are qualitatively similar to those described in cones by Baylor, Hodgkin & Lamb (1974*a*) and can probably be explained by attributing the sag from the spike to the plateau to a voltage-dependent, delayed increase in membrane conductance, for which there is some evidence (Schwartz, 1976).

In experiments similar to that illustrated by Fig. 4 it was found that the second flash was ineffective throughout the whole of the plateau but began to become effective when the rate of depolarization started to increase, i.e. at the first point of inflexion on the descending limb of the plateau.

Fig. 5 provides further evidence that the voltage during the plateau is saturated. Here a light, initially of intensity 2110 Rh*/sec was applied for 15 sec and then suddenly increased to 8960 Rh*/sec for a further 15 sec after which it was switched

off. The second step had no obvious immediate effect, either at 'on' or 'off', although the after-effect which lasted longer than with the 2110 Rh*/sec light alone showed that the second step did increase the concentration of internal transmitter.

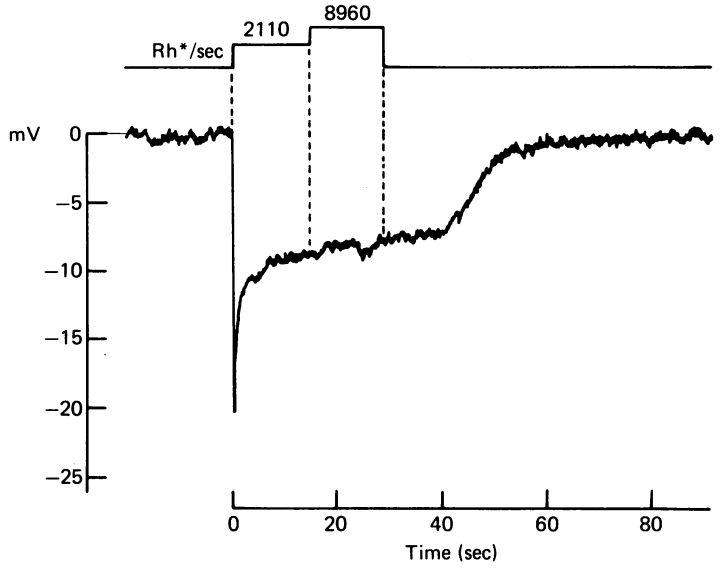

Fig. 5. Further evidence of saturation during the plateau. Note that increasing the light intensity from 2110 to 8960 Rh*/sec had no immediate effect. (Other records showed that the after-effect of the light of intensity 8960 Rh*/sec was more prolonged than that of the light of intensity 2110.)

Comparison of the response to large and small spots

From the continuous sheet model of a two-dimensional network of cells, the relation between the sensitivity and the radius of an illuminated circle should be given by eqn. (2·0) (see Lamb, 1976; Naka & Rushton, 1967; Schwartz, 1976):

$$\frac{S(a)}{S(\infty)} = 1 - \frac{a}{\lambda} K_1\left(\frac{a}{\lambda}\right), \tag{2.0}$$

where a is the radius, λ is the space constant, $K_1(\ )$ is a modified Bessel Function, $S(a)$ is the sensitivity to a spot of radius a and $S(\infty)$ is the limiting value of S when a is large compared to λ. In deriving eqn. (2.0) it is assumed that electrical spread in the rod network has reached a steady state, that both membrane and coupling impedances can be regarded as simple ohmic resistors and that the membrane resistance is unchanged by weak illumination. In the present experiments the radius of the small spot was usually 21·5 μm whereas that of the large spot was 570 μm; the apparent space constant for flashes was about 50 μm (see p. 229 for a qualification arising from the fact that λ is time-dependent). As can be seen from Table 3 the observed ratio of sensitivities averaged 0·094, whereas the value predicted by eqn. (2·0) was 0·117. If allowance is made for Gaussian light scattering with a scatter coefficient of $\sigma = 10$ μm, in approximate agreement with Schwartz (1973), Copenhagen

TABLE 3. Responses to large (570 μm radius) and small (21·5 μm radius) spots

	S_F^{ϕ}(mV/Rh*)		t_{peak}(sec)			$\frac{S_F^{\phi}(21{\cdot}5)}{S_F^{\phi}(570)}$		
	570 μm	21·5 μm	570 μm	21·5 μm	λ (μm)	observed	calc. (1)	calc. (2)
Rod	(1)	(2)	(3)	(4)	(5)	(6)	(7)	(8)
1	3·23	0·19	0·68	0·90	58	0·058	0·113	0·1004
2	3·36	0·16	0·81	0·94	71	0·074	0·084	0·0755
3	2·15	0·12	0·73	0·93	55	0·057	0·122	0·1080
4	0·415	0·047	0·78	1·12	55	0·113	0·122	0·1080
5	0·510	0·036	0·81	1·01	(50)	0·071	0·140	0·1229
6	0·780	0·18	0·56	0·74	48	0·224	0·148	0·1297
7	0·88	0·084	0·69	0·82	(50)	0·095	0·140	0·1229
8	2·00	0·189	1·00	1·30	(50)	0·094	0·140	0·1229
9	2·07	0·20	1·20	1·36	(50)	0·097	0·140	0·1229
10	1·80	0·15	1·16	1·40	(50)	0·083	0·140	0·1229
Mean	1·56	0·123	0·84	1·05		0·094	0·117	0·114

In column 5 the space constant λ was measured from the exponential decline of the peak of the flash response on either side of an illuminated strip. The over-all average value of 50 μm (based on thirty-eight rods) was used when no measurement of λ was made (these values are enclosed in parentheses). The ratios in column 7 were calculated from eqn. (2.0) and λ with no allowance for light scatter. Column 8 was calculated as in Schwartz (1976) with a scatter coefficient σ of 10 μm.

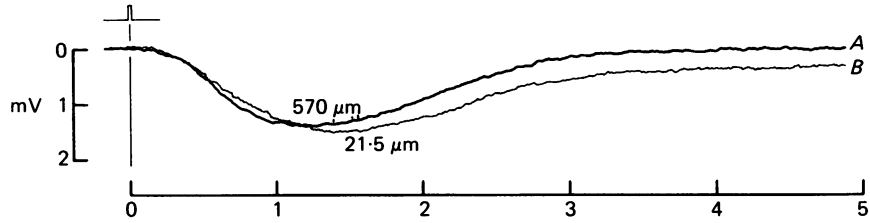

Fig. 6. Comparison of responses in linear region obtained with *A*, large spot (570 μm radius), and *B* small spot (21·5 μm radius). The strength of the 20 msec flash was 0·79 Rh*/rod in *A* and 8·06 Rh*/rod in *B*. (No allowance for light scatter.) Eighteen sweeps were averaged in *A* and nineteen in *B*.

& Owen (1976*a*) and Detwiler & Hodgkin (1979), the theoretical ratio becomes 0·114.

One would only expect eqn. (2.0) to hold if there were no conductance change during the response and both membrane and coupling impedances could be treated as ohmic. If these conditions held the form of the response to small and large spots should be identical. As can be seen from Fig. 1*B*, Fig. 6 and Table 3, this prediction was not fulfilled, for the response to a small spot reached a later maximum and was of greater duration than the response to a large spot. A further point is that the range of voltages over which the response is linear is less with the small spot than with the large, as would be expected if light intensity rather than voltage were largely responsible for desensitization. The difference illustrated by Figs. 1 and 6 was seen only if a very low flash repetition rate, about 1/20 sec, was employed.

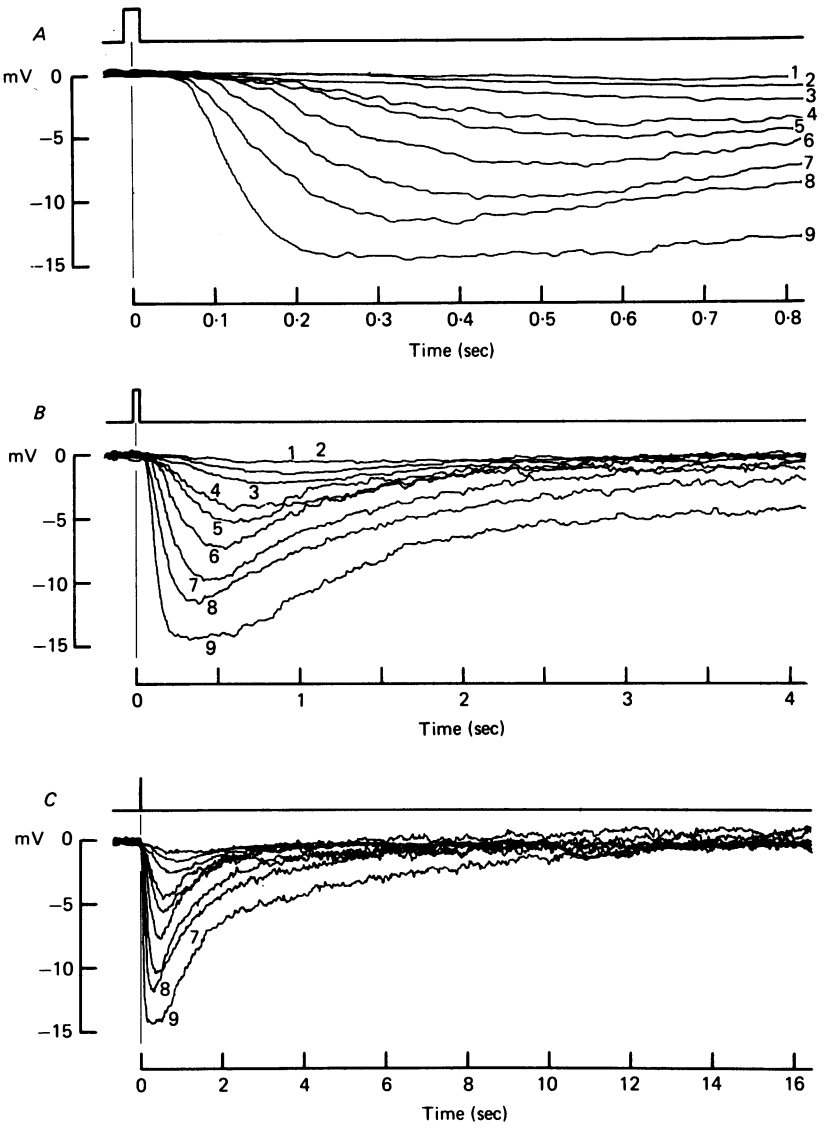

Fig. 7. Intensity series with a small spot (radius 21·5 μm) obtained on same rod as that in Fig. 3. The strength of the 20 msec flashes in Rh*/rod were: curves 1–5: 3·0, 7·3, 16, 39, 67; curves 6–9: 165, 388, 950, 4050.

Intensity series with small spots

Fig. 7 which is from the same rod as Figs. 1 and 3, completes the intensity series for the 21·5 μm radius spot. As Copenhagen & Owen (1976*a*) have found the initial spike is not seen at all with the small spot and, as other experiments showed, it could not be evoked when the flash intensity was increased 1–2 orders of magnitude beyond that in Fig. 7.

Fig. 8, which is taken from Figs. 3 and 7, compares the response to large and small spots with a strong flash. It shows, as does Fig. 4*A* of Copenhagen & Owen (1976*a*)

that although the initial spike is completely absent with the small spot, the plateau produced by the small spot at 0·5–1·0 sec is nearly as large as the plateau produced by the large one – about 90 % at 0·7 sec. If there were no light scatter and if the space constant did not change with light intensity one would expect eqn. (2·0) to apply over the whole range of light intensities, which it plainly does not, since it predicts a ratio of 0·085 for $S(21{\cdot}5)/S(\infty)$ as opposed to the observed value of 0·9. One way of accounting for this is to suppose that during the plateau, but not during the initial spike there is an increase in membrane conductance in the illuminated region. This would shorten

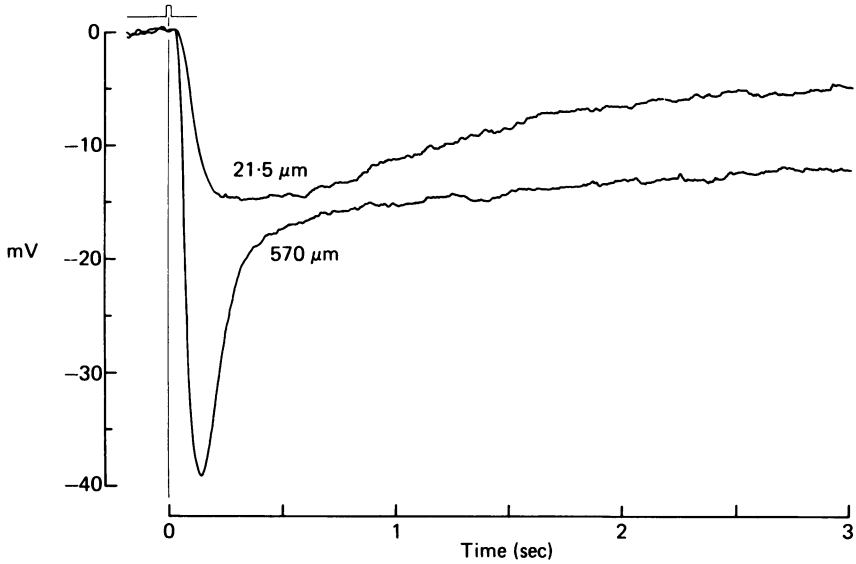

Fig. 8. Comparison of responses to strong flashes with large (570 μm radius) and small (21·5 μm radius) spots. The strength of the flash was 4050 Rh*/rod in both cases; from Figs 3 and 7.

the space constant and make the small spot relatively more effective during the plateau. Another possibility is that the result can be explained in terms of the combined effect of light scatter and non-linearity in the transduction mechanism, but we see no satisfactory way of developing such an argument quantitatively without an independent measurement of the light scattering function. The position is further complicated by the unexpected results to be described in the next section.

Electrical spread in the rod network

Electrical spread in the rod network was investigated by flashing a narrow strip of light onto the retina at varying distances from the impaled cell. This method was first employed by Lamb (1976) and Lamb & Simon (1976*a*) and has been used since by several authors (Detwiler *et al.* 1978; Leeper, Normann & Copenhagen, 1978). In *Pseudemys* and *Chelydra* it has been found that the peak of the electrical wave declines exponentially on either side of the illuminated strip with a space constant of about 25 μm in red-sensitive cones and approximately twice that value in rods (Lamb & Simon, 1976*a*; Detwiler *et al.* 1978). In the red-sensitive cones of both *Pseudemys* and

Chelydra Detwiler & Hodgkin (1979) found that moving the strip of light away from the impaled cone caused the response to become smaller and to reach a peak later. This is what is expected in a network where the connecting elements are resistive and each cone behaves like a resistance and capacity in parallel.

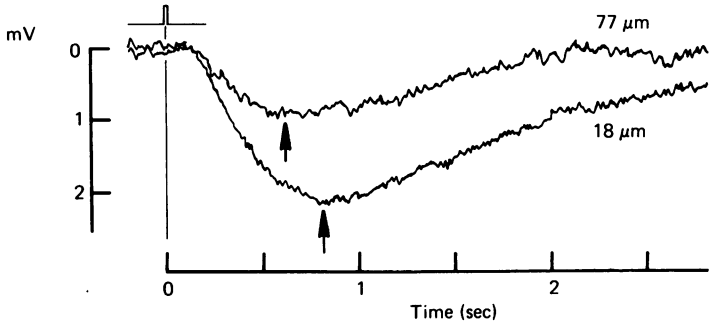

Fig. 9. Responses of rod to 20 msec flash which illuminated a strip of retina 1 mm × 19 μm wide at 18 μm (lower trace) and 77 μm (upper trace) from impaled rod. Twenty-two responses were averaged in the lower curve and ten in the upper curve. The intensity of the flash (without allowing for light scatter) was 3·1 photon μm^{-2} and the repetition rate was 1 in 20 sec; maximum hyperpolarization to a strong flash was 25 mV and sensitivity to a weak large field flash was 9·1 mV photon^{-1} μm^2.

Fig. 9 illustrates the surprising result that in the rods of *Chelydra* the crest occurs progressively earlier as the signal is attenuated by distance. The effect obviously cannot continue to times less than zero because this would require the response to precede the flash. However, over the range of distances where reliable measurements can be made, we have consistently obtained sets of points which are reasonably well fitted by two straight lines of negative slope, as in Fig. 10. In the experiments summarized in Table 4*A*, the velocity over the measurable range (usually about 80 μm) averaged -332 μm sec^{-1}. The corresponding figure for the crest velocity in the red-sensitive cones of *Pseudemys* is $+2700$ μm sec^{-1}.

The shortening of the time to peak as the signal is attenuated by distance in rods is unlikely to be due to scattered light since it occurred at distances greater than those over which light scattering is considered to be of major importance. A stronger argument is that the effect is in the opposite direction from that likely to be produced by scattered light. Increasing the intensity of a flash reduces the time to peak and, except with very strong flashes, shortens the whole response. On a light-scattering basis one would expect to find the slowest (and smallest) responses when the illuminated strip was remote from the impaled cell and the fastest (and largest) when it coincided with the impaled cell. This is the reverse of the result obtained experimentally.

The changes in wave form that take place in the rod network imply that the electrical effects of an absorbed photon spread out over a large area initially and then contract to a smaller area at long times. This is illustrated by Fig. 11 which shows that the potential wave spreads through the rod network with an apparent space constant of about 50 μm at 0·5 sec after the flash (curve 1) whereas later in the response (curve 2, 2·07 sec) the wave contracts down to about half the distance that it

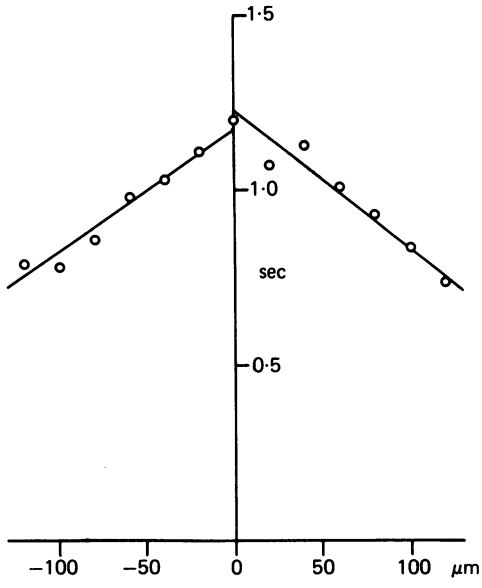

Fig. 10. Relation between the displacement of the strip of light from the impaled rod (plotted on the abscissa) and the time to peak of the response (ordinate). Note that the velocity is negative and has values of -291 μm/sec for negative displacements and -253 μm/sec for positive displacements. The traces from which this figure was made are illustrated in Fig. 13.

TABLE 4. Electrical spread in the rod network.

A. In darkness

Average (thirty-eight rods) peak space constant $\lambda_p = 48{\cdot}6 \pm 1{\cdot}7$ μm (S.E. of mean).
Average (twenty-eight rods) peak velocity $\theta_p = -332 \pm 31$ μm/sec (S.E. of mean).

B. With steady diffuse illumination

			λ_p (μm)		θ_p (μm/sec)	
Rod	Bkg (Rh*/sec)	S_F^R	Expt.	Model	Expt.	Model
(1)	(2)	(3)	(4)	(5)	(6)	(7)
1	—	1·0	35·9	—	−175	—
	1·6	0·38	35·9	—	−291	—
2	—	1·0	53·9	55.6	−211	−257
	2·41	0·32	55	65·5	−496	−665
	42·3	0·049	65·6	73	−1748	−1370

The peak space constant λ_p and the peak velocity θ_p were measured from the peak of the flash response on either side of an illuminated strip (cf. Figs. 10,11). For part *B*, the background was a 570 μm radius spot, wave-length 520 nm, intensity given in column 2, which caused the proportional reduction in sensitivity (S_F^R) shown in column 3. In columns 4–7 the experimentally observed values in one rod are compared with those predicted by the model (see Fig. 14) assuming that the only effect of the background is to alter the time course of the response.

previously occupied. In this case the potential curve crosses the zero axis at large distances and is markedly non-exponential so that the measurement of a space constant is impossible. Curve 3 gives the steady-state distribution calculated by superposition from the flash response and scaled so that its peak coincides with the other two; it is exponential outside the region where light is scattered and provides an average value of 27·5 μm for the space constant in the steady state.

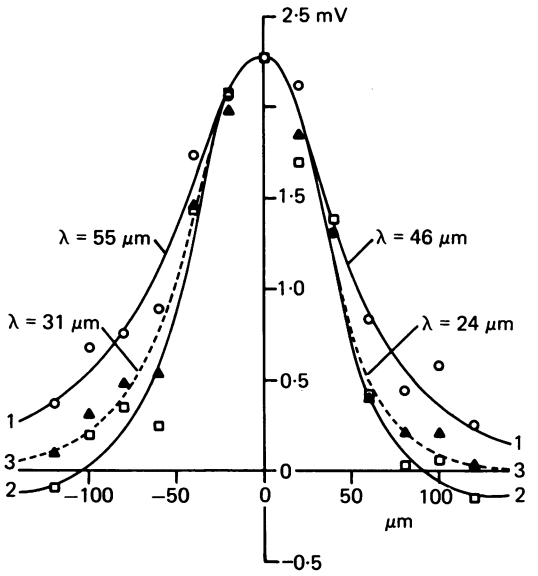

Fig. 11. 'Response contraction' illustrated by distribution of potential at different times after flash. Curve 1 (○) at 0·507 sec after flash; curve 2 (□) at 2·07 sec after flash; curve 3 (▲, interrupted line) steady state distribution calculated by integration of flash responses and normalized to the peak of the other two curves. Same experiment as Figs. 10 and 13.

It would be useful to make direct measurements of both the initial space constant and the steady-state space constant. However, direct measurement of the initial space constant is not possible because the voltage rises sufficiently slowly after a flash for appreciable relaxation of the space constant to have occurred before the voltage is large enough to be measurable. The steady state space constant could in principle be determined by measuring the spatial distribution of potential on either side of a steadily illuminated strip. However, responses which give voltages of more than a fraction of a mV under the slit desensitize rods so powerfully that scattered light reaching distant cells may have more effect than the electrical signal spreading through the network. We have therefore determined the steady state space constant by integrating flash responses to predict the response to a step in the absence of desensitization. These values of the steady state space constant are shown in Fig. 11. The average value of the space constant in the steady state is about one half of the space constant at the peak.

Possible explanations of the response contraction in rods

Illumination of the surround is known to produce a delayed depolarization in cones, by a mechanism involving horizontal cells (Baylor *et al.* 1971), and a similar recurrent inhibition might be responsible for the response contraction in rods. Two pieces of evidence argue against this.

(1) Narrow slits of the type used in the present experiments have little effect on horizontal cells, which collect over a large area.

(2) All horizontal cells which we have recorded from have an input from cones, so if the contraction of the rod response depends on horizontal cell activity one would expect a different effect at wave-lengths long enough to excite cones more than rods. In fact the response contraction was independent of the wave-length of the stimulating light.

For these reasons it is considered unlikely that L-type horizontal cells mediate the response contraction in rods. The effect might conceivably depend on a type of horizontal cell which receives only from rods, or on direct rod-to-rod inhibitory synapses, but in the absence of evidence for these possibilities we prefer to attribute response-contraction to the properties of the rod network itself. What is required is that the network should behave like a high-pass filter so that quick responses spread a long way and slow ones a short distance only. Such a characteristic might arise either from capacitative behaviour in the connexions between rods or from behaviour resembling an inductance in the rod membrane itself. Some evidence for the second possibility is provided by the fact that the voltage response of rods to rectangular currents of either sign shows an overshoot (Copenhagen & Owen, 1976*b*; Baylor & Fettiplace, 1977; Werblin, 1978).

Conductance changes resembling an inductance are well known in excitable cells where the delayed increase in K conductance (g_K) associated with depolarization gives an outward current which increases with time for a positive step and an inward current which increases with time for a negative step (see Cole & Baker, 1941; Hodgkin & Huxley, 1952). The changes in current are easier to understand if the step is positive than if it is negative. What happens in the second case is that hyperpolarization causes a delayed decrease in the standing outward potassium current and hence leads to an increase in the net inward current associated with the negative step. In the Appendix it is shown that for this system to mimic an inductance the internal potential V must be positive to the potassium equilibrium potential V_K ($V > V_K$). An apparent inductance also occurs if hyperpolarization causes a delayed increase in the conductance to an ion like Na with a reversal potential positive to the resting potential; in this case V must be negative to the equilibrium potential of the ion in question, e.g. $V < V_{Na}$.

Analysis of electrical spread in the rod network

The rod network is a two-dimensional array but if it is activated by a long strip of light it can be treated as a one-dimensional cable, as in Fig. 12.

In the Appendix it is shown that under certain conditions a membrane which undergoes voltage-dependent conductance changes behaves as though it contained an inductance. An equivalent circuit, which is shown by the transverse elements in

Fig. 12, consists of a parallel resistance, r_1 and an inductance l in series with a resistance r_2. The membrane capacity c has been omitted because the rod response is so slow that the RC time constant can be neglected.

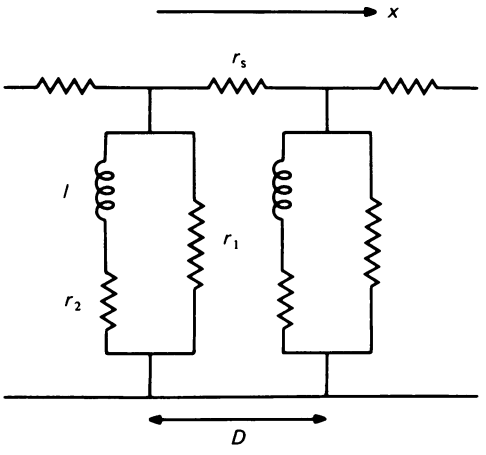

Fig. 12. Model of retina used in considering one dimensional electrical spread in rod network. x, direction at right angles to illuminated strip; D, distance between rods (taken as 20 μm); r_s coupling resistance between rods (about 250 MΩ if square array assumed); l apparent inductance of single rod (about 10^9 Henry); r_1 and r_2 membrane resistances in parallel and series with inductance (about 2000 and 600 MΩ respectively).

The relation between the voltage, V, and membrane current, i, in a single rod is

$$\tau \frac{\mathrm{d}i}{\mathrm{d}t} + i = \tau g_\infty \frac{\mathrm{d}V}{\mathrm{d}t} + V g_0, \tag{3.1}$$

where τ is the time constant of the conductance change under conditions of constant voltage; g_∞ is the high frequency conductance and g_0 is the low frequency conductance.

$$g_\infty = g_1 = 1/r_1$$

$$g_0 = g_1 + g_2 = \frac{r_1 + r_2}{r_1 r_2}$$

$$\tau = l g_2$$

In fitting the model to the experimental results it was assumed that the rods are arranged in a square array with the strip of light at $x = 0$ and parallel to one side of the squares. The current at the nth rod was then calculated from

$$i_n r_s = V_{n+1} - 2V_n + V_{n-1} \tag{3.2}$$

Details of the numerical method used in solving eqns. (3.1) and (3.2) are given in the next section. However, before going into this it is useful to consider the analytical solutions which can be obtained when a sinusoidal voltage is applied to the continuous analogue of the lumped cable shown in Fig. 12. For a continuous sheet fed by a slit at right angles to x eqns. (3.1) and (3.2) become

$$\tau \frac{\partial I}{\partial t} + I = \tau G_1 \frac{\partial V}{\partial t} + V(G_1 + G_2) \tag{3.3}$$

and

$$IR_s = \frac{\partial^2 V}{\partial x^2} \tag{3.4}$$

where I is the membrane current density, R_s is the sheet resistivity, G_1 is the high frequency conductance of the membrane per unit area and (G_1+G_2) is the low frequency conductance per unit area; L is the inductance × unit area and $\tau = LG_2$. If there are D^2 rods per unit area, $G_1 = g_1/D^2$, $G_2 = g_2/D^2$ and $L = lD^2$; in a square array the sheet resistivity $R_s = r_s$, the resistance of a single coupling element.

Eqns. (3.3) and (3.4) can be combined to give

$$\lambda_\infty^2\left(\tau\frac{\partial}{\partial t}+1\right)\left(\frac{\partial^2 V}{\partial x^2}\right) = \tau\frac{\partial V}{\partial t} + V\rho, \tag{3.5}$$

where λ_∞, the space constant at high frequencies, is given by $\lambda_\infty = (R_sG_1)^{-\frac{1}{2}}$

and

$$\rho = \frac{G_1+G_2}{G_1}.$$

With the boundary condition $V = V_0e^{j\omega t}$ at $x = 0$ the solution of (3.5) is

$$V = V_0 \exp\{j\omega t-(\alpha+j\beta)|x|\}, \tag{3.6}$$

where

$$(\alpha^2+2\alpha\beta j-\beta^2)\lambda_\infty^2 = \frac{j\omega\tau+\rho}{j\omega\tau+1}. \tag{3.7}$$

On separating eqn. (3.7) into its real and imaginary parts and solving for α and β we find

$$\alpha = \frac{1}{2^{\frac{1}{2}}\lambda_\infty}[A+\sqrt{A^2+B^2}]^{\frac{1}{2}} \tag{3.8}$$

$$\beta = -\frac{1}{2^{\frac{1}{2}}\lambda_\infty}[-A+\sqrt{A^2+B^2}]^{\frac{1}{2}}, \tag{3.9}$$

where

$$A = \frac{\rho+\omega^2\tau^2}{1+\omega^2\tau^2} \quad \text{and} \quad B = \frac{\omega\tau(1-\rho)}{1+\omega^2\tau^2}.$$

Eqn. (3.6) may also be written

$$V = \exp(-|x|/\lambda_\omega)\exp[j\omega(t-|x|/\theta)], \tag{4.0}$$

where λ_ω is the space constant and θ the phase velocity at a frequency ω

$$\lambda_\omega = \alpha^{-1} \tag{4.1}$$

and

$$\theta = \omega\beta^{-1} \tag{4.2}$$

Eqns. (3.8) and (3.9) lead to values of velocity and λ_ω which are of the same order of magnitude as those calculated by more elaborate methods described in the next section.

The following simplifications apply in limiting cases.

(i) If $\omega \to \infty$, then $\beta \to 0$ and $\alpha^{-1} = \lambda_\infty = (R_sG_1)^{-\frac{1}{2}}$.

(ii) If $\omega \to 0$, then $\alpha = \lambda_0{}^{-1}$, and $\beta \to 0$ as

$$\beta = -\frac{\tau\omega}{2\lambda_0}\left(\frac{\rho-1}{\rho}\right), \tag{4.3}$$

so that

$$\theta = -\frac{2\lambda_0}{\tau}\left(\frac{\rho}{\rho-1}\right), \tag{4.4}$$

where λ_0 is the low frequency space constant given by

$$\lambda_0 = [(G_1+G_2)R_s]^{-\frac{1}{2}}. \tag{4.5}$$

(iii) If $G_1 \to 0$ and $G_2 \to \infty$, the original differential equation simplifies to

$$\frac{\partial^3 V}{\partial x^2 \partial t} = \frac{R_s V}{L} \tag{4.6}$$

for which (4.0) is the appropriate solution with

$$\theta = -\lambda_\omega \omega \tag{4.7}$$

and

$$\lambda_\omega = (2\omega L/R_s)^{\frac{1}{2}}. \tag{4.8}$$

Responses of the rod network: numerical solutions

(i) *Electrical spread in one dimension.* The voltage at the nth rod in the one-dimensional cable shown in Fig. 12 is given by the following differential equation, obtained by combining eqns. (3.1) and (3.2):

$$\tau(\Delta^2 - g_\infty r_s)\dot{V}_n = -(\Delta^2 - g_0 r_s)V_n, \tag{5.1}$$

where $\dot{V}_n = \dfrac{dV_n}{dt}$ and the operator Δ^2 has the meaning

$$\Delta^2 V_n = V_{n-1} - 2V_n + V_{n+1} \tag{5.2}$$

When a known voltage V_0 is presented at rod number 0 and the cable is assumed to be terminated at rod $r+1$ by a short-circuit, the voltage at the intervening rods is given by a system of coupled differential equations derived from eqn. (5.1). It is convenient to write these equations in a band-matrix form

$$\tau \begin{pmatrix} a & 1 & 0 & 0 & \dots & \dots \\ 1 & a & 1 & 0 & \dots & \dots \\ 0 & 1 & a & 1 & \dots & \dots \\ \dots & \dots & \dots & \dots & \dots & \dots \\ 0 & 0 & \dots & \dots & 1 & a \end{pmatrix} \begin{pmatrix} \dot{V}_1 \\ \dot{V}_2 \\ \dot{V}_3 \\ \dots \\ \dot{V}_r \end{pmatrix} = - \begin{pmatrix} b & 1 & 0 & 0 & \dots & \dots \\ 1 & b & 1 & 0 & \dots & \dots \\ 0 & 1 & b & 1 & \dots & \dots \\ \dots & \dots & \dots & \dots & \dots & \dots \\ 0 & 0 & \dots & \dots & 1 & b \end{pmatrix} \begin{pmatrix} V_1 \\ V_2 \\ V_3 \\ \dots \\ V_r \end{pmatrix} - \begin{pmatrix} V_0 + \tau \dot{V}_0 \\ 0 \\ 0 \\ \dots \\ 0 \end{pmatrix}, \tag{5.3}$$

where $a = -(g_\infty r_s + 2)$ and $b = -(g_0 r_s + 2)$.

In shorthand this matrix equation is

$$\tau A \dot{V} = -BV - C, \tag{5.4}$$

where A and B are $r \times r$ matrices, and $\dot{V}$, V and C are $r \times 1$ matrices. Inverting matrix A we obtain

$$\tau \dot{V} = -A^{-1}BV - A^{-1}C. \tag{5.5}$$

This system of coupled differential equation can be solved by standard procedures (see below).

(ii) *Electrical spread in two dimensions.* The method outlined above can also be extended to solve a two-dimensional network of rods. A square lattice of rods was chosen, although the method is equally applicable to any configuration of connexions. For a square lattice an equation similar to (5.1) describes the behaviour of voltage:

$$\tau(\Delta_x^2 + \Delta_y^2 - g_\infty r_s)\dot{V}_{m,n} = -(\Delta_x^2 + \Delta_y^2 - g_0 r_s)V_{m,n}, \tag{5·6}$$

where

$$(\Delta_x^2 + \Delta_y^2)V_{m,n} = V_{m+1,n} + V_{m-1,n} + V_{m,n+1} + V_{m,n-1} - 4V_{m,n}. \tag{5.7}$$

Only a one eighth plane bounded (for instance) by the lines $y = 0$ and $x = y$ need be solved for the case of a square lattice, since voltages over the rest of the plane can be deduced from considerations of symmetry. For convenience the two-dimensional numbering system, $V_{m,n}$,

was converted into a one-dimensional system, V_k, where $k = m(m+1)/2+n$, by renumbering the rods from the origin in zig-zag fashion over the entire one eighth plane out to the boundary of the array:

0
1 2
3 4 5
6 7 8 9

The differential equation for rod 4, for instance, is then obtained from eqn. (5.6):

$$\tau\{\dot{V}_2+\dot{V}_3+\dot{V}_5+\dot{V}_7-(g_\infty r_s+4)\dot{V}_4\} = -\{V_2+V_3+V_5+V_7-(g_0 r_s+4)V_4\}.$$

A system of similar equations for the whole array can be written down in matrix form in a manner analogous to eqns. (5.3) and (5.4). Matrix A can then be inverted and the solution obtained as outlined above.

Computations were carried out in double-precision arithmetic on an IBM 370 machine with the aid of standard FORTRAN subroutines from the Numerical Algorithms Group (NAG) library. Systems of coupled differential equations were solved using routine D02ABF (Merson's method) to an accuracy of 1 part in 10^{10} and matrix inversions were performed using routine F01AAF (Crout's method). The main limitation on accuracy in the systems of coupled rods arose because an infinite array is approximated by a finite number of rods terminated by a short-circuit. The adequacy of this approximation was checked by progressively increasing the distance of the short-circuit termination from the origin until no significant change in the solution occurred; in both one-dimensional and two-dimensional simulations a distance of 15 rods between origin and short-circuit termination was found to be sufficient for typical values of the parameter λ_∞/D of around 3.

The accuracy of the solutions for both one- and two-dimensional systems of coupled rods could be checked by comparing the sum of the voltages over all elements of the array with the voltage produced by injecting the same current into a single rod. These two voltages, which by the arguments on p. 218, eqns. (1.1)–(1.3), should be equal at all times, in practice agreed to within 0·25% of the peak voltage. The one-dimensional solution was checked in two further ways: (i) by applying a step voltage and verifying that the steady-state solution was that expected for a lumped resistive cable (Detwiler & Hodgkin, 1979); (ii) by applying sinusoidal voltages of various frequencies and checking for close agreement with the solutions obtained for a continuous cable in eqns. (3.6)–(3.9) (exact agreement is not expected since the responses of lumped and continuous cables are not identical, but when the steady-state space constant λ_0 is greater than the cell spacing the discrepancy is not large).

Comparison between experimental and computed responses

The equations developed above for one-dimensional cables driven by slits of light do not apply to those parts of the rod network which receive a direct current input resulting from the effects of scattered light. The extent of scattered light in experiments was judged by observing where the decay of peak response as a function of distance became approximately exponential, as expected for an unilluminated cable; in the experiment shown in Fig. 11, for example, the responses at $|x| \geqslant 40$ μm satisfy this criterion. To compare the responses in this experiment with the predictions of the model, therefore, the voltage responses at $x = \pm 40$ μm were taken as the driving voltages at the origin of the cable shown in Fig. 12. Voltages at rods further away from the slit of light could then be predicted for particular values of the cable parameters λ_0, λ_∞ and τ. Of these three parameters only λ_0, the steady state space constant, could be determined directly, by integrating the slit responses over time to obtain the response to steady illumination in the absence of desensitization. The remaining two parameters, λ_∞ and τ, were determined by using linear interpolation between

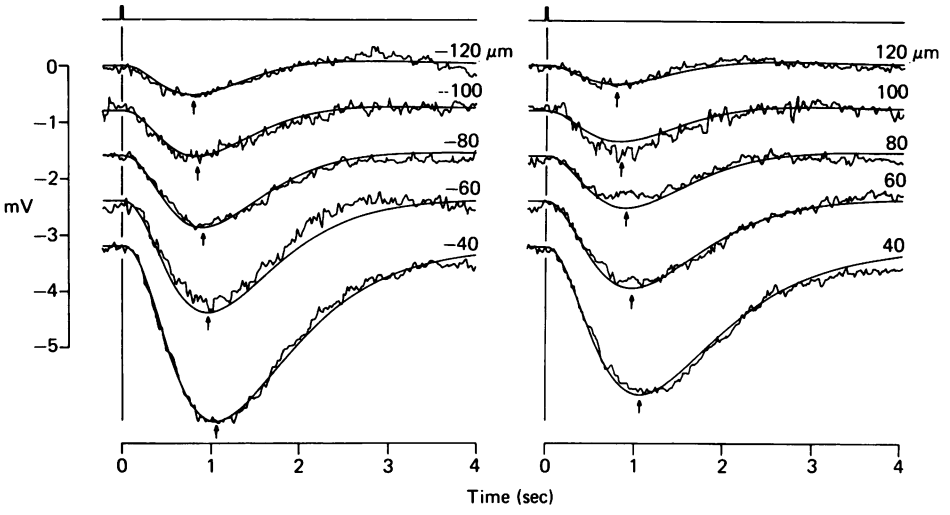

Fig. 13. An example of fitting the model described in the text to the responses of a rod to slit flashes of light. The noisy traces are either single responses or the average of two responses to a strip of light (width 19 μm, wave-length 520 nm, intensity 1·16 photon μm^{-2}, flash duration 20 msec) flashed at various distances, shown in μm alongside each trace, away from the impaled rod. The space constants of the peak response were 45 μm (left panel) and 38·4 μm (right panel) and the space constants of the steady response (see Fig. 11) were 30·8 μm and 24·3 μm. Velocities of the peak response were -291 μm/sec and -253 μm/sec (see Fig. 10). Maximum hyperpolarization was 26·5 mV; sensitivity to a weak diffuse flash was 31 mV photon^{-1} μm^2; temperature 18·5 °C; resting potential -42 mV. The continuous lines show the action of the inductive properties of the membrane on rod responses. An empirical equation of form

$$V = A(\exp(-\alpha t) - \exp(-\beta t))^{n-1}$$

was fitted to the responses at ± 40 μm; λ_0 was taken at its measured value of 30·8 and 24·3 μm; the parameters λ_∞ and τ were adjusted until the experimental values of peak space constant and peak velocity were reproduced. Values of λ_∞ and τ thus obtained were 65·1 μm and 1·32 sec (left panel), and 52·7 μm and 1·80 sec (right panel). The peaks of the responses predicted using these values of λ_∞ and τ are marked with an arrow.

trial values until the experimentally measured quantities λ_p (the space constant of the peak response) and θ (the peak velocity) were accurately reproduced.

An example of the predictions of the model fitted to a series of experimental traces is shown in Fig. 13. Most of the divergence of the model from the experimental traces seems to be due to variations in the experimental response amplitude as a function of distance, perhaps because the rods are clustered rather than forming the regular network assumed in the model.

Slightly different values of the parameters λ_∞, λ_0 and τ were required to fit responses to slits flashed either side of the rod. The average values from both sides were $\lambda_\infty = 59$ μm, $\lambda_0 = 27{\cdot}7$ μm and $\tau = 1{\cdot}51$ sec.

The effect of background illumination on electrical spread

The effect of background illumination on the spread of the peak response in two rods is shown in Table 4. The response spreads slightly further on a background,

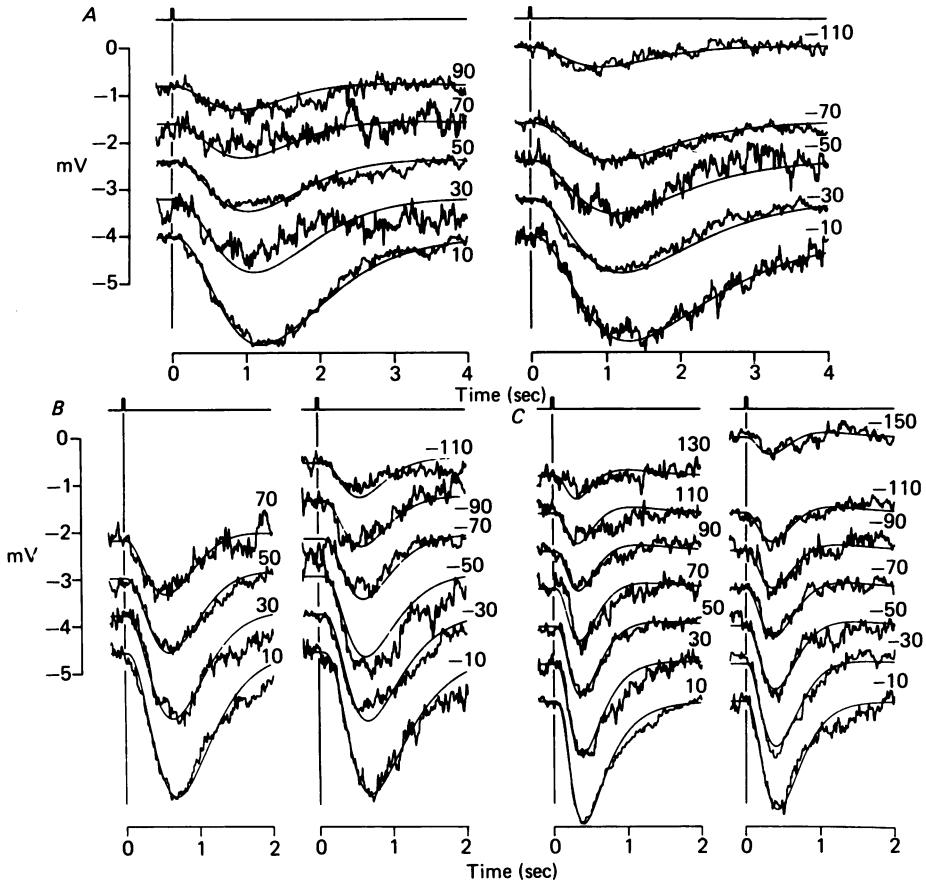

Fig. 14. The effects of light adaptation on the responses of a rod to slit flashes of light, compared with the predictions of the model. *A* responses in darkness. Conditions as in legend to Fig. 13, except that the strip flash intensity was 2·8 photon μm^{-2}. Maximum hyperpolarization 22·5 mV; sensitivity to a weak diffuse flash 5·5 mV photon^{-1} μm^2; temperature 20·2 °C; resting potential −43 mV. The smooth lines were calculated by a similar method to that given in the legend to Fig. 13, except that values of λ_∞ = 100 μm and τ = 1·5 sec were used for both panels. The space constant and peak velocity of the experimental and computed peak responses are given in Table 4. *B*, responses on a dim full-field background, which hyperpolarized the cell by 0·5 mV. Slit flash intensity was 11·8 photon μm^{-2}; other experimental conditions as in *A*. Continuous traces calculated using the same values of λ_∞, λ_0 and τ as in *A*, but with new empirical functions for the responses at ± 10 μm. Space constants and peak velocities given in Table 4. *C*, responses on a moderate full-field background, which hyperpolarized the cell by 2 mV. Slit flash intensity was 64 photon μm^{-2}. Smooth traces calculated as in *A*, *B*. Space constants and peak velocities given in Table 4.

which could indicate a light-dependent decrease in membrane conductance. However, the response is much faster in the presence of steady illumination (Baylor & Hodgkin, 1974), so it seems equally possible that the more rapid response allows less relaxation of membrane conductance, and hence the peak will 'sample' a space constant closer to λ_∞. Fig. 14 supports this second possibility; values of λ_∞, λ_0 and τ which had given a good fit to responses in darkness also provided a fit within experimental error to responses on dim and moderate backgrounds.

The variability of the response of rods to weak flashes

The variability of the response to flashes was studied by exposing the retina to a series of identical weak flashes spaced at intervals of 10–20 sec. The increment in voltage variance was computed as a function of time and compared with the mean voltage response. Table 5 and Fig. 15, which illustrates an experiment of this kind, show that there are two main differences from the result expected if rods were isolated: first, the variance change is much less than that calculated from the flash sensitivity on the assumption that rods are isolated, and second the peak of the variance curve occurs later than the peak of the voltage curve.

TABLE 5. The variability of the response to flashes

	Run	Number of flashes	$\bar{q}$ (Rh*)	$\bar{U}$ (mV)	S_F^ϕ $\left(\frac{mV}{Rh^*}\right)$	$\Delta\sigma^2$ (mV^2)	ρ (observed)	ρ (calc.)	$\frac{t_{\sigma^2}}{t_U}$
	(1)	(2)	(3)	(4)	(5)	(6)	(7)	(8)	(9)
A	1	6	0·49	2·6	5·24	0·24	0·017	0·014	1·67
	2*	7	0·49	2·0	4·07	< 0·07	< 0·009	(0·014)	—
	3*a**	18	0·70	2·1	3·10	0·06	0·009	(0·014)	1·38
	3*b**	11	0·46	1·4	3·10	0·06	0·014	(0·014)	1·37
	4*a*	26	0·70	1·8	2·54	0·14	0·031	(0·014)	1·29
	4*b**	20	0·70	1·6	2·34	0·07	0·019	(0·014)	1·22
	5*	32	0·71	1·5	2·15	0·08	0·025	0·023	1·17
B	6*a**	23	1·92	2·0	1·03	0·14	0·069	(0·014)	1·08
	6*b**	19	1·92	2·0	1·02	0·04	0·021	(0·014)	1·42
	7*	21	3·14	1·7	0·54	0·05	0·057	0·021	1·55
	8	19	4·2	1·7	0·39	0·13	0·198	(0·014)	1·12
Mean		20	1·49	1·8	2·15	0·10	0·048	0·016	1·33
Mean, *A*		19	0·63	1·7	3·08	0·11	0·019	0·016	1·35
Mean, *B*		20	2·80	1·9	0·76	0·09	0·086	0·016	1·29

$\bar{q}$ is the mean number of photoisomerizations per rod in each flash; $\bar{U}$ is the mean peak hyperpolarizations; S_F^ϕ is flash sensitivity ($= \bar{U}/\bar{q}$); $\Delta\sigma^2$ is the increase in variance at peak U; $\rho = \Delta\sigma^2(U)/\Delta\sigma^2(U)_{isol}$. Column 7 observed ρ; column 8 ρ calculated by the method of Lamb & Simon (1976) from the space constant which had values of 50, 39 and 41 μm in runs 1, 5 and 7; elsewhere the mean λ of 50 μm was used and ρ is given in parentheses. The last column is the ratio of the time to peak variance to the time to peak voltage. In column 1 *a*, *b*, etc. indicate two runs on the same rod; a * indicates that responses were filtered with a high-pass filter of time constant 10 sec. The peak variance was on average 1·4 times the variance at peak U. Rods have been divided into two groups, *A* and *B*, on the basis of their flash sensitivity, and separate means computed for each group. Run 2, in which there was no significant variance change, has not been included in the means. The ratio of peak variance to variance in darkness varied between 1·8 and 4·4 (excluding run 2) and averaged 2·7.

If there were no coupling the increase in variance as a function of time, $\Delta\sigma^2_{isol}(t)$, could be calculated from the relation

$$\Delta\sigma^2_{isol}(t) = \bar{q}[V^\phi(t)]^2, \tag{6.1}$$

where $\bar{q}$ is the mean number of photo-isomerizations per rod, each of which would produce a voltage $V^\phi(t)$ in an isolated rod. In deriving eqn. (6.1) it is assumed that the response is in the linear range, that q is a Poisson variable with variance equal to mean and that all rods have identical sensitivities. When the variance change is measured at the time of peak hyperpolarization (t_{peak}) eqn. (6.1) becomes

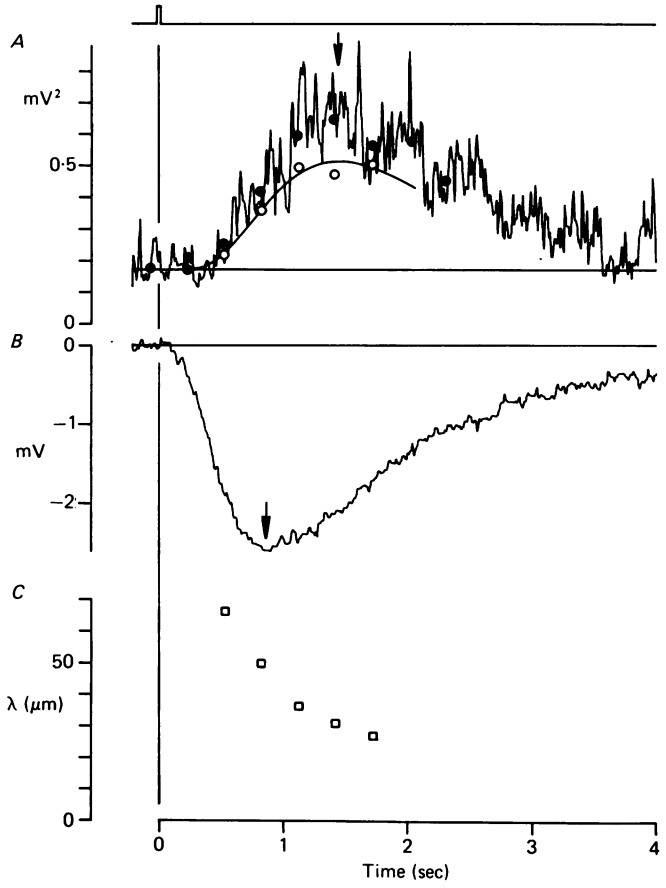

Fig. 15. The variability of the response in a sensitive cell (rod 1 in Table 5) to a series of dim flashes. *A*, the variance as a function of time after six diffuse flashes delivering on average 0·49 Rh* per rod. The filled circles show the average value of variance in successive time intervals of 300 msec; the standard error of each of these variance averages is less than the size of the circle. The estimated peak variance increase is marked with an arrow. The open circles and solid line show the variance calculated from the space constant obtained in *C*, as described in the text. *B*, the average hyperpolarization as a function of time. The peak hyperpolarization is marked with an arrow. *C*, the space constant as a function of time measured from a series of strip flashes (cf. Fig. 11). Maximum hyperpolarization 38·5 mV; sensitivity to a weak diffuse flash 71·3 mV photon^{-1} μm^2, or 5·24 mV/Rh*; temperature 19·3 °C.

$$\begin{aligned} \triangle\sigma^2_{\text{isol}}(t_{\text{peak}}) &= \bar{q}[S^{\phi}_{\text{F}}]^2 \\ &= \bar{U}^2/\bar{q} \end{aligned} \tag{6.2}$$

where $\bar{U}$ is the mean peak hyperpolarization.

In the experiment of Fig. 15 the variance calculated from eqn. 6.2) was 13·5 mV^2, as against an observed variance of 0·235 mV^2 at the time of the peak hyperpolarization. Hence the ratio $\rho(t)$ defined by

$$\rho(t) = \frac{\triangle\sigma^2(t)}{\triangle\sigma^2_{\text{isol}}(t)} = \frac{\triangle\sigma^2(t)}{\bar{q}[V^{\phi}(t)]^2} \tag{6.3}$$

had a value of 0·0174 at the time of the peak hyperpolarization. The value of ρ increased somewhat at later times, but did not exceed 0·125. Values of $\rho(t_{\text{peak}})$ obtained in other experiments of a similar kind are given in Table 5, column 7, and are all much less than unity, the mean value being about 0·05. This confirms the conclusions of Fain (1975), Schwartz (1976) and Gold (1979) that the variability of rod responses is much less than if each rod were isolated from its neighbours. Fig. 15 and Table 5 also show that the variance peak was often later than the peak hyperpolarization, which by eqn. (6.3) implies that the ratio ρ is increasing with time. In other words, the variability of the response increases with time after a flash. The reasons for this surprising observation will be explored below.

The effects of coupling on the variability of the rod response can be allowed for as follows. Let $V^{\phi}_{m,n}(t)$ be the voltage produced at the impaled rod by a single photo-isomerization in the rod whose coordinates in the network are (m,n). Then the variance of the voltage contribution from this rod, when a series of diffuse flashes deliver on average $\bar{q}$ photo-isomerizations per rod, is $\bar{q}[V^{\phi}_{m,n}(t)]^2$ (cf. eqn. (6.1)). Since the variance contribution from each cell is independent the variance contribution from each cell in the network can be summed to give the total variance at the impaled cell:

$$\triangle\sigma^2(t) = \bar{q} \sum_{m,n} [V^{\phi}_{m,n}(t)]^2. \tag{6.4}$$

Substituting this result in eqn. (6.3) we obtain the following expression for the behaviour of ρ;

$$\rho(t) = \frac{\sum_{m,n} [V^{\phi}_{m,n}(t)]^2}{[V^{\phi}(t)]^2}. \tag{6.5}$$

This expression for ρ is similar to that derived by Lamb & Simon (1976*a*) for random noise in a coupled network; in their paper it is called $\sigma^2/\sigma^2_{\text{isol}}$, and has been calculated in their Fig. 3 for the case of a pure-resistive square network. Strictly speaking the Lamb–Simon theory is not applicable to the rod network, which contains reactive membrane conductances, but it can be shown that it provides a reasonable approximation at times up to and including the peak rod response, that is while the decline of potential away from a slit source is observed to approximate to the exponential decline found in a resistive network. Thus in the theoretical case considered in Fig. 17 (p. 238) the Lamb-Simon theory gives a value for ρ which is within about 10% of that obtained from eqn. (6.5) at 1·2 sec.

It is interesting to compare the observed values of ρ at the time of peak hyperpolarization with those plotted by Lamb & Simon in their Fig. 3. For this purpose we need estimates of λ'/D where λ' is the space constant at the time of the peak hyperpolarization and D is the effective distance between rods which was taken as 20 μm. In three experiments λ' was measured directly from the decline of potential on either side of an illuminated strip; in the other experiments the mean value of $\lambda' = 50$ μm determined from the spatial decline of the peak in 41 rods was employed.

Comparison of columns 7 and 8 in Table 5 show that there is approximate agreement between observed and calculated values of ρ in the more sensitive rods ($S^{\phi}_{\text{F}} > 2$ mV) but in two rather insensitive cells the observed variance was much greater than that expected from photon noise in a coupled network. The discrepancy

may be worse than appears from Table 5 because allowance for non-linearity (see Katz & Miledi, 1972) might increase the observed value of ρ by 10–20%. The most likely explanation of the discrepancy between observed and calculated variances is that there are other sources of variability besides photon noise, for example differences in the sensitivity of adjacent rods, which would make the observed variance larger than that calculated by the Lamb–Simon theory.

In those cases where the observed variance was much higher than that calculated there was usually little delay between the peaks of the voltage and variance curves. Thus in rod 5 the first run gave a small delay and a large variance whereas the second run, determined 10 min later, gave a large delay and a small variance close to that calculated for photon noise. This would be explained if (1) the delay is a characteristic of photon noise, and (2) another source of response variability was present in the first but not the second set of measurements. Several rods gave apparently large increases in variance which were regarded as spurious (and have been excluded from Table 5) because there was clear evidence of a drift in sensitivity during the run. In these cases the peak of the variance usually coincided with the peak hyperpolarization.

The high-pass filter characteristic of the rod network accounts satisfactorily for the fact that the peak of the variance curve occurs later than the peak hyperpolarization in those rods where photon noise was the major source of response variability. In a previous section (pp. 228 and 229) it was shown that the value of the space constant at 0·5 sec after a flash might be two or three times greater than the value 1·5 sec later. Since the ratio ρ increases as λ decreases the falling phase of $U(t)$ should be noisier than the rising phase and the peak variance should occur later than the peak hyperpolarization.

In Fig. 15 the lower graph shows how the apparent values of λ decreased with time in the experiment under consideration; these measurements were determined in the usual way by flashing a narrow strip of light at different distances from the impaled rod. The open circles in the upper part of the Figure show the theoretical values of variance calculated by Lamb & Simon's theory from these measured values of λ. The theory clearly accounts very satisfactorily for the observation that the variance maximum occurs later than the peak potential.

Two rods in which there was a substantial delay between the peak potential and the peak variance illustrate a neat consequence of the high-pass characteristic of the rod network. When a sensitive rod is exposed to a series of identical large-field flashes the photons that affect it are absorbed in a random way over a disc with a radius of 50–100 μm. A consequence of the high-pass filter characteristic of the rod network is that the photons absorbed at a distance from the impaled cell should give faster as well as smaller responses than those absorbed close to it. This prediction is borne out by Fig. 16*A* (obtained on the same very sensitive rod as Fig. 15) which shows that the two smallest responses in a train of 6 are faster than the two largest responses. Another experiment illustrating the same point with a larger number of trials but using a less sensitive cell is given in Fig. 16*B*.

One can see without resorting to any detailed theory that the results in Figs. 15 and 16 are consistent because the difference between the two sets of responses in Fig. 16, which determines the variance, is greatest some time after the average time of the maximum. Hence the variance peak is delayed as in Fig. 15.

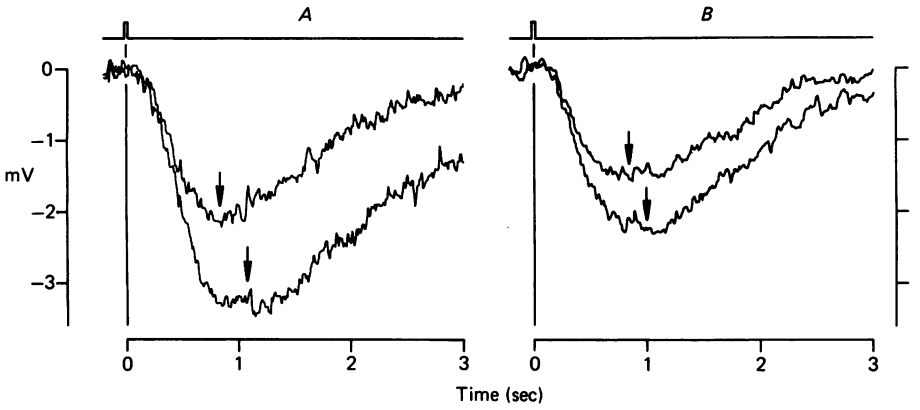

Fig. 16. The difference in shape between the smaller and larger responses to a series of identical diffuse flashes. *A*, the smaller trace is the average of the two smallest individual responses, and the larger trace the average of the two largest, in the series of six responses used to construct Fig. 15. *B*, the smaller trace is the average of the eight smallest individual responses, and the larger the average of the eight largest, to a series of twenty-one responses to diffuse flashes each delivering on average 1·72 Rh* per rod. The smaller and larger responses were found to be distributed randomly through the series. Maximum hyperpolarization 32 mV; sensitivity to a weak diffuse flash 0·46 mV/Rh*; temperature 19·6 °C.

DISCUSSION

The evidence that the rod network has some of the properties of a high-pass filter has a number of implications which need to be considered.

Differences between current and voltage wave forms

(i) *Small signals.* In Fig. 17*A* we have used eqn. (3.1) to predict the time course of the current generated by a rod outer segment in response to one photoisomerization. The curve labelled 'voltage' is the mean voltage response to a weak diffuse flash causing on average one photoisomerization per rod, and the curve labelled 'photocurrent' is the current required to generate such a response if eqn. (3.1) holds and g_0, g_∞ and τ have values consistent with the spread of potential on either side of an illuminated strip. This calculation is approximate because it assumes that the rod outer segments act as a perfect current source, that is have a resistance much higher than the inner segments. Allowance for the resistance of the outer segment would make the current and voltage curves diverge even more than in this figure.

Some evidence for the view that rod currents last longer than the average voltage response is provided by the difference between the time course of the currents observed by Baylor, Lamb & Yau (1979*b*) in response to weak flashes and the small voltage signals observed by other workers using rods from the same animal (Fain, 1976; Cervetto *et al.* 1977).

The difference between the voltage and current wave forms illustrated in Fig. 17 helps to explain the different time courses of the voltage responses to large and small spots. For the sake of argument suppose that the electrical properties of the rod membrane approximate to those of an inductance and that the conductance g_1 is zero

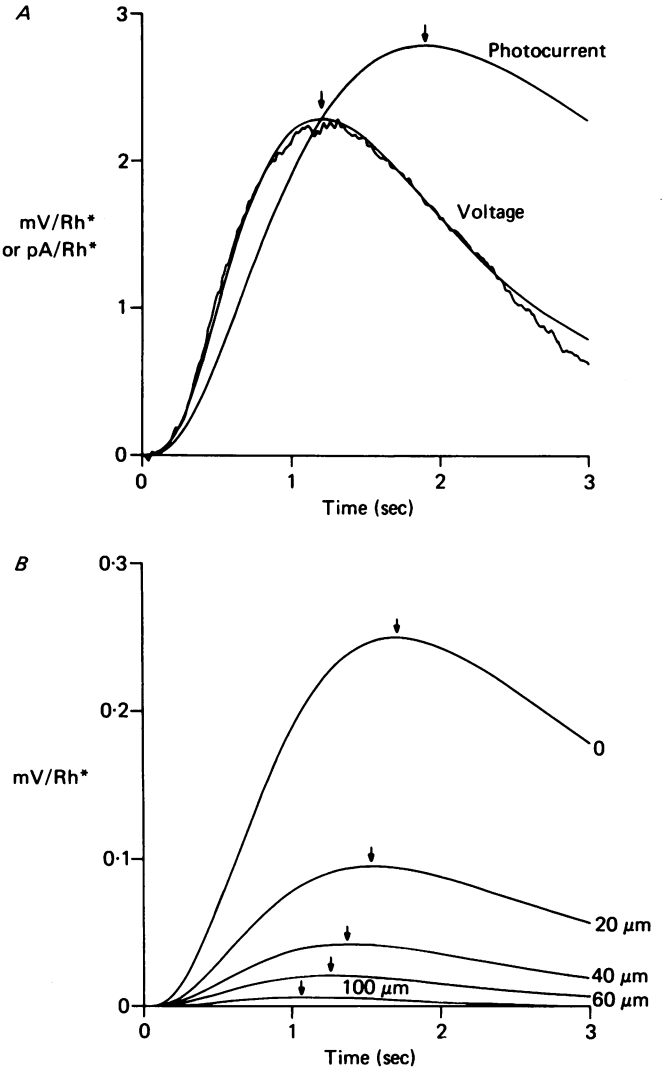

Fig. 17. *A*, the noisy trace shows the average hyperpolarization, in response to a series of dim diffuse flashes, of the rod whose responses to strip flashes are illustrated in Fig. 13. The response has been scaled to show the voltage produced by a single photoisomerization. The continuous curve near the experimental trace is an empirical function of the form noted in the legend to Fig. 13. The photocurrent has been calculated from this function by integrating eqn. (3.1) using the following circuit parameters: r_s = 253·6 MΩ; r_1 = 2225 MΩ; r_2 = 625 MΩ; l = 944 MH. These circuit values have been calculated from the average λ_∞, λ_0 and τ obtained in Fig. 13 by demanding that the DC input resistance of the square network be 80 MΩ (Owen & Copenhagen, 1977). The peak voltage is at 1·21 sec, and the peak photocurrent is at 1·91 sec. *B*, the curves show the voltage produced at increasing distances (shown alongside each curve) away from a rod which has received a single photoisomerization. Rods were assumed to form a square network, and the method outlined in the text, pp. 233 and 234, was used to obtain the voltage when the photocurrent shown in part *A* of this Figure was injected into an infinite network with circuit parameters as given above. The time to peak voltage at each position illustrated is: 0 μm, 1·71 sec; 20 μm, 1·53 sec; 40 μm, 1·37 sec; 60 μm, 1·26 sec; 100 μm, 1·06 sec.

and g_2 is infinite. When a large area is illuminated the voltage wave-form should then be the first derivative of the current and should reach a peak much earlier than the rod current. On the other hand with a small spot the impedance on which the rod current acts should be determined more by the coupling resistances between rods than by the impedance z_m of the rods themselves. Thus the input resistance of a two-dimensional network varies roughly as $r_s^{\frac{1}{2}} r_m^{\frac{1}{2}}$ for $\lambda/D = 2$–3 (Lamb & Simon, 1976*a*, Fig. 3). If the input resistance were purely resistive the voltage and current wave forms should be proportional to one another. This line of reasoning suggests that the voltage response to a small spot should last longer than to a large spot. In Fig. 17*B* the voltage produced when the photocurrent shown in Fig. 17*A* is injected into one rod in a square network has been calculated at various distances from the rod receiving illumination, and bears out these arguments: the voltage in the illuminated rod lasts considerably longer than when a large area is illuminated. The peak voltage in response to diffuse illumination was at 1·21 sec, and the calculated peak response to illumination of a single rod is at 1·71 sec, broadly in line with the results in Table 3 which show that the small spot peak was reached about 25% later than the large spot peak. A smaller effect in experiments would be expected since the small spot was 43 μm in diameter and probably stimulated several rods. Fig. 17 also shows that the ratio of peak voltage produced when a single rod is illuminated to the peak voltage when all are illuminated is 0·109, compared to an average ratio of 0·094 in Table 3. As the distance between the rod receiving illumination and the recording site is increased, the calculation in Fig. 17*B* shows that the voltage response becomes both smaller and faster, as was observed in Fig. 16.

The difference between the time course of the response to large and small spots, which we have observed consistently, does not agree with the results of Schwartz (1976) who found that for small signals, spots less than 100 μm in diameter gave the same time course as those from spots with a diameter of 1000 μm. The discrepancy may be connected with the fact that as in other early recordings from rods (e.g. Baylor & Hodgkin, 1973) the retinae used by Schwartz were 1/10–1/20 as sensitive as those used in the present work, an effect now attributed to over-exposure to light while setting up the preparation. The importance of using a low flash repetition rate (1/15–1/30 sec^{-1}) must also be stressed.

(ii) *Large signals.* The experiments of Baylor, Lamb & Yau (1979*a*) show that the current wave form injected by the outer segment after a strong flash consists of a rapid rise to a plateau followed by an exponential decline to the dark level. If many rods are illuminated by a strong flash the internal potential of the inner segment has a similar wave-form except that the plateau of -15 mV is preceded by a spike of -30 to -40 mV. This is true both in *Chelydra serpentina* and in *Bufo marinus*, the animal from which Baylor *et al.* (1979*a*) obtained their recordings (see Fain, 1976; Cervetto *et al.* 1977).

The occurrence of the initial spike is qualitatively consistent with the presence of an inductive reactance in the membrane, for if a differentiated component is added to the records of Baylor *et al.* (1979*a*) we should expect to obtain something very like the voltage response of rods when stimulated with a large area flash. By the argument used in the previous section this also explains why 40 μm diameter spots give a

plateau without a spike and why relatively large spots of 100 μm diameter or more are required to give an initial hyperpolarizing spike (cf. Figs. 3 and 7 of this paper and Copenhagen & Owen, 1976*a*).

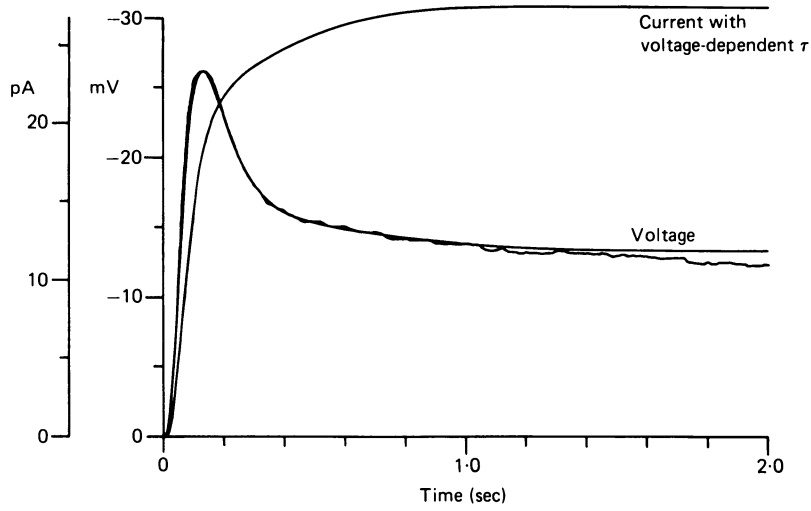

Fig. 18. The noisy trace labelled 'voltage' shows the maximum response to a bright diffuse flash of the rod whose responses were illustrated in Fig. 13. The smooth curve near the experimental trace is an empirical function, from which the photocurrent has been obtained by integrating eqn. (3.1). When the circuit parameters shown in the legend of Fig. 17 were used the current had a biphasic appearance, but if the time constant, τ were assumed to depend on voltage a flat-topped current similar to that observed when the saturating current is recorded from single rods (Yau, Lamb & Baylor, 1977, Baylor, 1977) can be obtained. The saturating current shown (labelled 'current with voltage-dependent τ') is calculated assuming that τ is halved at a potential 9 mV negative to the dark level.

In Fig. 18 the experimental voltage response to a large-field saturating flash has been used in eqn. (3.1) to predict the saturating photocurrent. When the values of $r_1 = 2225\ \mathrm{M}\Omega$ $r_2 = 625\ \mathrm{M}\Omega$ and $\tau = 1{\cdot}51$ sec which were obtained for potentials near the resting level (see Fig. 13) were used in eqn. (3.1), the current was found to have a biphasic time course unlike that seen by Baylor *et al.* (1979*a*). A reasonable current waveform can be obtained, however, if the time constant at the plateau is assumed to be less than at the resting potential; the curve labelled 'current' in Fig. 18 was computed on the basis that a 9 mV hyperpolarization reduced τ to one half, and is consistent with that described by Baylor *et al.* (1979*a*). The assumption that τ is voltage-dependent is arbitrary, but not implausible since the time constants of conductance changes are usually voltage dependent.

In the Appendix it is shown that the inductive reactance required to account for our observations on electrical spread in the rod network can be explained if hyperpolarization causes either a delayed increase in the conductance of an ion like sodium with an equilibrium potential positive to the resting potential, or a delayed decrease in the conductance of an ion like potassium with an equilibrium potential negative to the resting potential. The recent experiments of Bader, MacLeish & Schwartz

(1978) on isolated rods which show both inward and outward rectification suggest that both mechanisms may be present. Further evidence for the presence of both systems comes from a comparison of the results of Owen & Copenhagen (1977) on *Chelydra* with those of Fain, Quandt, Bastian & Gerschenfeld (1978) on *Bufo*. Thus the former group found lower resistances with depolarizing than with hyperpolarizing currents, as would be expected if depolarization increased K conductance, whereas the latter group's observations of the spike-plateau phenomenon suggest that hyperpolarization caused a delayed increase in Na conductance which was blocked by Cs. A large increase in Na conductance at the plateau would help to explain why a 43 μm diameter spot gave nearly the same sized plateau as a large spot of similar intensity (Figs. 3 and 8, and p. 226). There might be advantages in having two systems since this could help to keep the inductance relatively constant over a wide range of membrane potentials. Thus if both Na and K conductances were involved the contribution of Na towards the inductance would increase with hyperpolarization whereas that of K would decrease. However, all there arguments are somewhat indirect and the identification of the ionic mechanisms underlying voltage-dependent conductance changes in photoreceptors would seem to be an important objective for future research.

Difference between time course of voltage and its variance in response to a flash

Response contraction which results in the apparent space constant being greater at short than at long times after a flash accounts satisfactorily for the observation that the variance peak occurs later than the voltage peak (Fig. 15). It also explains the observation in some experiments that out of a series of responses to the same intensity flash the larger responses lasted longer than the smaller ones. This would be expected if the photons absorbed near the impaled cell give larger and longer responses than those absorbed at a distance.

The possible function of response contraction and receptor coupling

Electrical coupling between receptors may have the function of reducing the variability of responses at the expense of spatial acuity. This may allow animals to be aware of large objects at low levels of illumination even though they may not be able to resolve much detail.

The usefulness of electrical coupling would seem to be much increased by the high-pass filter characteristics of the rod syncytium which imply that the electrical effects of an absorbed photon cover a wide area initially and then contract down to a relatively smaller area at a later time. Subsequent retinal elements could take advantage of the changing spatial distribution of the photon signal in the receptors by averaging over either distance or time. Pathways with a large receptive field would observe the small signal containing the high frequency components of the photon response spreading over a large number of receptors. As a consequence these pathways would be more capable of detecting rapid changes in illumination and would have better temporal resolution than pathways with a small receptive field. This line of reasoning is supported in part by psychophysical studies showing that the critical frequency for flicker fusion increases with the area illuminated (e.g. Granit & Harper, 1930).

Retinal pathways may also vary with respect to integration time. Since the area covered by the photon signal is smaller late in time than early on, it follows that pathways with a long integration time will have better spatial resolution than those with a short integration time.

APPENDIX

Representation of time-dependent conductance changes by circuit containing an inductance

It is well known that membranes show inductance-like properties if hyperpolarization decreases the conductance of an ion like K with an equilibrium potential negative to the resting potential, or if it increases the conductance of an ion like Na with an equilibrium potential positive to the resting potential. If the driving force on the ion is reversed, that is if $V < V_K$ or $V > V_{Na}$ in the examples quoted above, then the circuit behaves as though it contained a large capacity.

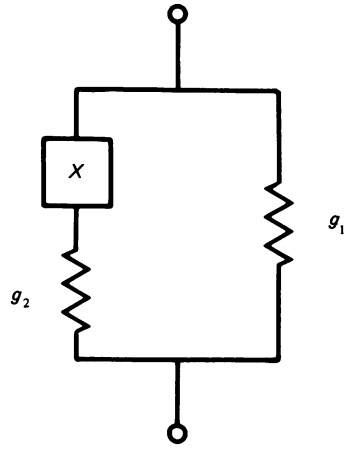

Fig. 19. Equivalent circuit of conductance changes. X may be either an inductance l or a capacity c; g_1 and g_2 are conductances.

These general conclusions can be proved in the following way for systems which obey kinetics of the kind described by Hodgkin & Huxley (1952) and Cole (1972).

Consider first the circuit in Fig. 19 where X may be either an inductance l or a capacity c. If i is the total current into the network, V is the potential difference across it and g_1 and g_2 are the conductances of the elements shown then the following equation applies both to case (1) where X is an inductance and to case (2) where X is a capacitance.

$$\tau \frac{\mathrm{d}i}{\mathrm{d}t} + i = \tau g_\infty \frac{\mathrm{d}V}{\mathrm{d}t} + V g_0, \tag{1.0}$$

where τ is the time constant of the current i under voltage clamp conditions, g_∞ is the limiting conductance at high frequencies and g_0 is the limiting conductance at low frequencies (i.e. d.c.). The meanings of τ, g_∞ and g_0 are different in the two cases, thus:

Case (1)

$$\begin{aligned} X &= l \text{ (inductance)} \\ \tau &= lg_2 \\ g_\infty &= g_1 \\ g_0 &= g_1+g_2 \end{aligned} \tag{1.1}$$

and case (2)

$$\begin{aligned} X &= c \text{ (capacitance)} \\ \tau &= c/g_2 \\ g_\infty &= g_1+g_2 \\ g_0 &= g_1 \end{aligned} \tag{1.2}$$

We shall now show that eqn. (1.0) also applies for small perturbations to systems where ionic conductances vary with time and membrane potential and conform to equations of the Hodgkin & Huxley type. Thus if the current i_j carried by the jth ionic species is determined by

$$i_j = (V-V_j)g_j \tag{2.0}$$

where V_j is the equilibrium potential of the jth ion and g_j is its ionic conductance which for small perturbations obeys the equation

$$\frac{\tau \mathrm{d}g_j}{\mathrm{d}t}+g_j = f(V) \tag{2.1}$$

where $f(V)$ is any continuous function of voltage; τ may also be a voltage dependent but is taken as a constant for small perturbations. Let $i_j = \bar{i}_j + \triangle i_j$, $V = \bar{V} + \triangle V$, $g_j = \bar{g}_j + \triangle g_j$, etc., where the bar indicates the mean or steady-state value of the variable and $\triangle$ is its perturbation. Then neglecting second order quantities such as $\triangle V \triangle g_j$ eqn. (2.0) becomes

$$\triangle i_j = (\bar{V}-V_j)\triangle g_j + \bar{g}_j \triangle V \tag{2.2}$$

and (2.1) becomes

$$\tau \frac{\mathrm{d}(\triangle g_j)}{\mathrm{d}t} + \triangle g_j = f'(\bar{V})\triangle V, \tag{2.3}$$

where

$$f'(V) = \mathrm{d}[f(V)]/\mathrm{d}V$$

On combining (2.2) and (2.3) and remembering that $\bar{g}_j = f(\bar{V})$ we obtain

$$\tau \frac{\mathrm{d}}{\mathrm{d}t}(\triangle i_j) + \triangle i_j = \bar{g}_j \tau \frac{\mathrm{d}(\triangle V)}{\mathrm{d}t} + [(\bar{V}-V_j)f'(\bar{V})+f(\bar{V})]\triangle V \tag{2.4}$$

Since the steady-state current $\bar{i}_j$ is given by

$$\bar{i}_j = (\bar{V}-V_j)f(\bar{V}) \tag{2.5}$$

the limiting slope conductance at low frequencies is given by

$$g_0 = \frac{\partial \bar{i}_j}{\partial \bar{V}} = (\bar{V}-V_j)f'(\bar{V})+f(\bar{V}) \tag{2.6}$$

By definition, eqn. (2·0), the limiting conductance at high frequencies, g_∞, equals $\bar{g}_j$.

Hence eqn. (2.4) can be written in the same form as (1.0), i.e.

$$\tau \frac{\mathrm{d}}{\mathrm{d}t}(\Delta i_j) + \Delta i_j = g_\infty \tau \frac{\mathrm{d}(\Delta V)}{\mathrm{d}t} + g_0 \Delta V, \tag{2.7}$$

where

$$g_\infty = \bar{g}_j \tag{2.8}$$

and

$$g_0 = (\bar{V} - V_j) \frac{\partial \bar{g}_j}{\partial \bar{V}} + \bar{g}_j \tag{2.9}$$

From this it is evident that the equivalent circuit in Fig. 19 applies for small perturbations and that X will behave like an inductance if $g_0 > g_\infty$ which requires that the term $(V - V_j)\, \partial \bar{g}_j / \partial V$ be positive, whereas it behaves like a capacitance if $g_0 < g_\infty$ and $(V - V_j)\, \partial \bar{g}_j / \partial V$ is negative.

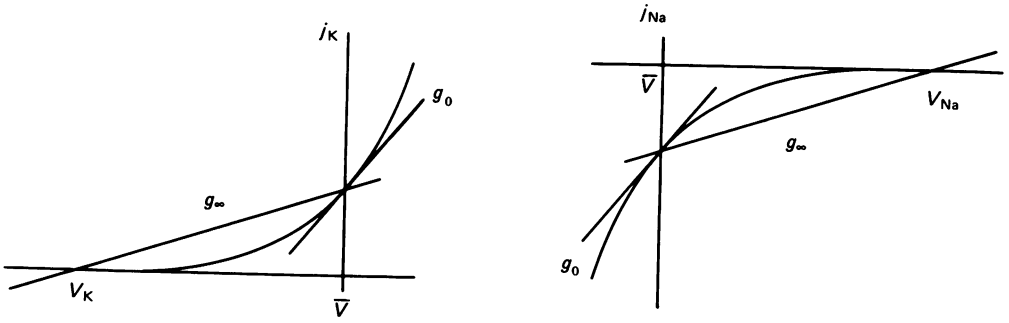

Fig. 20. Two ways in which time-dependent conductance changes can mimic an inductance. Note that the chord and tangent of the curve at $\bar{V}$ have slopes g_∞ and g_0 respectively.

Under conditions of constant voltage the current approaches its equilibrium value with a time constant $\tau (= lg_2$ or $c/g_2)$ whereas under conditions of constant current the time constant is $(g_\infty/g_0)\, \tau$.

Fig. 20 illustrates the two ways in which an inductance may arise at a potential $\bar{V}$. In A where the ionic species is considered to be K both $(V - V_K)$ and $\partial g_K / \partial V$ are positive; in B where the ionic species might be Na both $(V - V_{Na})$ and $\partial g_{Na} / \partial V$ are negative. A necessary consequence of the hypothesis is that if the membrane is to show inductance-like behaviour at the resting potential there must be some standing current through the voltage-dependent conductance. Thus in case A where $\bar{V} > V_K$ a steady outward K current is balanced by a steady inward current of some other ion like Na. The conductance to the other ion is in parallel with g_1 so that the eqn. (1.0) and the equivalent circuit in Fig. 19 are still correct descriptions of the electrical properties of the membrane.

Fig. 20 also shows why the conductances g_0 and g_∞ are sometimes called slope and chord conductances respectively.

This investigation was supported in part by a grant EY02048 from the National Eye Institute, U.S.P.H.S., and grant G.975/425/N from the M.R.C., U.K. We are indebted to Drs T. D. Lamb, W. G. Owen and V. Torre for reading the manuscript and for helpful comments. Our thanks are also due to Mr R. H. Cook for designing and building equipment.

REFERENCES

BADER, C. R., MACLEISH, P. R. & SCHWARTZ, E. A. (1978). Responses of solitary rod photoreceptors isolated from tiger salamander retina. *Proc. natn. Acad. Sci. U.S.A.* **75**, 3507–3511.

BAYLOR, D. A. & FETTIPLACE, R. (1975). Light path and photon capture in turtle photoreceptors. *J. Physiol.* **248**, 433–464.

BAYLOR, D. A. & FETTIPLACE, R. (1977). Kinetics of synaptic transfer from receptors to ganglion cells in turtle retina. *J. Physiol.* **271**, 425–448.

BAYLOR, D. A., FUORTES, M. G. F. & O'BRYAN, P. M. (1971). Receptive fields of single cones in the retina of the turtle. *J. Physiol.* **214**, 265–294.

BAYLOR, D. A. & HODGKIN, A. L. (1973). Detection and resolution of visual stimuli by turtle photoreceptors. *J. Physiol.* **234**, 163–198.

BAYLOR, D. A. & HODGKIN, A. L. (1974). Changes in time scale and sensitivity in turtle photoreceptors. *J. Physiol.* **242**, 729–758.

BAYLOR, D. A., HODGKIN, A. L. & LAMB, T. D. (1974*a*). The electrical responses of turtle cones to flashes and steps of light. *J. Physiol.* **242**, 685–727.

BAYLOR, D. A., HODGKIN, A. L. & LAMB, T. D. (1974*b*). Reconstruction of the electrical responses of turtle cones to flashes and steps of light. *J. Physiol.* **242**, 759–791.

BAYLOR, D. A., LAMB, T. D. & YAU, K.-W. (1979*a*). The membrane current of single rod outer segments. *J. Physiol.* **288**, 589–611.

BAYLOR, D. A., LAMB, T. D. & YAU, K.-W. (1979*b*). Responses of retinal rods to single photons. *J. Physiol.* **288**, 613–643.

CERVETTO, L., PASINO, E. & TORRE, V. (1977). Electrical responses of rods in the retina of *Bufo marinus*. *J. Physiol.* **267**, 17–51.

COLBURN, T. R. & SCHWARTZ, E. A. (1972). Linear voltage control of current passed through a micropipette with variable resistance. *Med. Electron. & biol. Engng* **10**, 504–509.

COLE, K. S. (1972). *Membranes, Ion and Impulses*, London: University of California Press.

COLE, K. S. & BAKER, R. F. (1941). Longitudinal impedance of the squid giant axon. *J. gen. Physiol.* **22**, 649–670.

COPENHAGEN, D. R. & OWEN, W. G. (1976*a*). Functional characteristics of lateral interactions between rods in the retina of the snapping turtle. *J. Physiol.* **259**, 251–282.

COPENHAGEN, D. R. & OWEN, W. G. (1976*b*). Coupling between rod photoreceptors in a vertebrate retina. *Nature, Lond.* **260**, 57–59.

DETWILER. P. B. & HODGKIN, A. L. (1979). Electrical coupling between cones in turtle retina. *J. Physiol.* **291**, 75–100.

DETWILER, P. B., HODGKIN, A. L. & MCNAUGHTON, P. A. (1978). A surprising property of electrical spread in the network of rods in the turtle's retina. *Nature, Lond.* **274**, 562–565.

FAIN, G. L. (1975). Quantum sensitivity of rods in the toad retina. *Science, N.Y.* **187**, 838–841.

FAIN, G. L. (1976). Sensitivity of toad rods: dependence on wave-length and background illumination. *J. Physiol.* **261**, 71–101.

FAIN, G. L., GOLD, G. H. & DOWLING, J. E. (1976). Receptor coupling in the toad retina. *Cold Spring Harb. Symp. quant. Biol.* **40**, 547–561.

FAIN, G. L., QUANDT, F. N., BASTIAN, B. L. & GERSCHENFELD, H. M. (1978). Contribution of a caesium-sensitive conductance increase to the rod photopresponse. *Nature, Lond.* **272**, 467–469.

GOLD, G. H. (1979). Photoreceptor coupling in retina of the toad *Bufo marinus*. II. Physiology. *J. Neurophysiol.* **42**, 311–328.

GRANIT, R. & HARPER, P. (1930). Comparative studies on the peripheral and central retina. II. Synaptic reaction in the eye. *Am. J. Physiol.* **95**, 211–228.

HODGKIN, A. L. & HUXLEY, A. F. (1952). A quantitative description of membrane current and its application to conduction and excitation in nerve. *J. Physiol.* **117**, 500–544.

JACK, J. J. B., NOBLE, D. & TSIEN, R. W. (1975). *Electric Current Flow in Excitable Cells*, p. 91. Oxford: Clarendon Press.

KATZ, B. & MILEDI, R. (1972). The statistical nature of the acetylcholine potential and its molecular components. *J. Physiol.* **224**, 665–699.

LAMB, T. D. (1976). Spatial properties of horizontal cell responses in the turtle retina. *J. Physiol.* **263**, 239–255.

LAMB, T. D. & SIMON, E. J. (1976*a*). The relation between intercellular coupling and electrical noise in turtle photoreceptors. *J. Physiol.* **263**, 257–286.

LAMB, T. D. & SIMON, E. J. (1976*b*). Analysis of electrical noise in turtle cones. *J. Physiol.* **263**, 257–286.

LEEPER, H. F., NORMANN, R. A. & COPENHAGEN, D. R. (1978). Evidence for passive electrotonic interactions in red rods of toad retina. *Nature, Lond.* **275**, 234–236.

NAKA, K.-I. & RUSHTON, W. A. H. (1967). The generation and spread of S-potentials in fish (*Cyprinidae*). *J. Physiol.* **192**, 437–461.

OWEN, W. G. & COPENHAGEN, D. R. (1977). Characteristics of the electrical coupling between rods in the turtle retina. In *Vertebrate Photoreception*, ed. BARLOW, H. B. & FATT, P. London: Academic Press.

SCHWARTZ, E. A. (1973). Responses of single rods in the retina of the turtle. *J. Physiol.* **232**, 503–514.

SCHWARTZ, E. A. (1975). Rod-rod interaction in the retina of the turtle. *J. Physiol.* **246**, 617–638.

SCHWARTZ, E. A. (1976). Electrical properties of the rod syncytium in the retina of the turtle. *J. Physiol.* **257**, 379–406.

WERBLIN, F. S. (1978). Transmission along and between rods in the tiger salamander retina. *J. Physiol.* **280**, 449–470.

YAU, K.-W., LAMB, T. D. & BAYLOR, D. A. (1977). Light-induced fluctuations in membrane current of single toad rod outer segments. *Nature, Lond.* **269**, 78–80.